Highlights

Assessing the contribution of groundwater to catchment travel time distributions through integrating conceptual flux tracking with explicit Lagrangian particle tracking

Miao Jing, Rohini Kumar, Sabine Attinger, Qi Li, Chunhui Lu, Falk Heße

- We provide an integrated analysis of susburface travel times by coupling flux tracking with particle tracking.
- Travel times in a central European catchment show various degrees of spatial and temporal variabilities in soil zone and groundwater aquifer.
- Catchment mean travel time is vulnerable to biased groundwater characterization due to the tailing behavior.
- We recommend to use multiple summary statistics to provide a robust description of catchment travel time distribution.

Assessing the contribution of groundwater to catchment travel time distributions through integrating conceptual flux tracking with explicit Lagrangian particle tracking

Miao Jing[a,b,c,d,*], Rohini Kumar[d,**], Sabine Attinger[d,e], Qi Li[c,f], Chunhui Lu[a,b], Falk Heße[d,e,]

[a] *State Key Laboratory of Hydrology-Water Resources and Hydraulic Engineering, Hohai University, 210098 Nanjing, China*
[b] *Yangtze Institute for Conservation and Development, Hohai University, 210098 Nanjing, China*
[c] *State Key Laboratory of Geomechanics and Geotechnical Engineering, Institute of Rock and Soil Mechanics, Chinese Academy of Sciences, 430071 Wuhan, China*
[d] *Department of Computational Hydrosystems, Helmholtz Centre for Environmental Research – UFZ, Permoserstr. 15, 04318 Leipzig, Germany*
[e] *Institute of Earth and Environmental Sciences, University of Potsdam, Karl-Liebknecht-Str. 24–25, 14476 Potsdam, Germany*
[f] *University of Chinese Academy of Sciences, Beijing, China*

Abstract

Travel time distributions (TTDs) provide an effective way to describe the transport and mixing processes of water parcels in a subsurface hydrological system. A major challenge in characterizing catchment TTD is quantifying the travel times in deep groundwater and its contribution to the streamflow TTD. Here, we develop and test a novel modeling framework for an integrated assessment of catchment scale TTDs through explicit representation of 3D-groundwater dynamics. The proposed framework is based on the linkage between a flux tracking scheme with the surface hydrologic model (mHM) for the soil-water compartment and a particle tracking scheme with the 3D-groundwater model OpenGeoSys (OGS) for the groundwater compartment. This linkage provides us with the ability to simulate the spatial and temporal dynamics of TTDs in these different hydrological compartments from grid scale to regional scale. We apply this framework in the Nägelstedt catchment in central Germany. Simulation results reveal that both shape and scale of grid-scale groundwater TTDs are spatially heterogeneous, which are strongly dependent on the topography and aquifer structure. The component-wise

[*] mjing@live.cn
[**] falk.hesse@ufz.de
rohini.kumar@ufz.de

analysis of catchment TTD shows a time-dependent sensitivity of transport processes in soil zone and groundwater to driving meteorological forcing. Catchment TTD exhibits a power-law shape and fractal behavior. The predictive uncertainty in catchment mean travel time is dominated by the uncertainty in the deep groundwater rather than that in the soil zone. Catchment mean travel time is severely biased by a marginal error in groundwater characterization. Accordingly, we recommend to use multiple summary statistics to minimize the predictive uncertainty introduced by the tailing behavior of catchment TTD.

Keywords: Travel time distribution, Flux tracking, Particle tracking, Coupled model, Predictive uncertainty

1. Introduction

Characterizing the travel or transit time (TT) of a water parcel is important for the assessment and management of global and regional water resources. Travel time distributions (TTDs) provide a statistical representation of this property by accounting for the storage, mixing, and transport processes in a hydrologic system (Niemi, 1977; McGuire and McDonnell, 2006; Botter et al., 2010; McDonnell et al., 2010). Analysis of water parcel TTs is, therefore, of high relevance to the groundwater recharge estimation (Cartwright et al., 2017; McCallum et al., 2017), the vulnerability of water resources (Molnat and Gascuel-Odoux, 2002; Benettin et al., 2015), and the assessment of nonpoint-source agricultural contamination (Böhlke and Denver, 1995; Eberts et al., 2012; Kumar et al., 2020).

Water TTs are typically not measured directly. Instead, they are inferred using models constrained by hydrological and geochemical data (McCallum et al., 2014; McGuire et al., 2007; Benettin et al., 2019). Such models of TTDs can be classified into lumped parameter models, dynamic StorAge Selection (SAS) functions, flux tracking models, and particle tracking models (Sprenger et al., 2019). Among them, the SAS approach is a state-of-art technique to characterize the temporal dynamics of TTDs and mixing processes of water parcels (Botter et al., 2011; Rinaldo et al., 2015; Harman, 2015). It distinguishes between the TTDs and residence time distributions (RTDs; Botter et al. (2011)) by virtue of said SAS functions and is able to comprehensively describe the age-specific outflow generation. Moreover, two different forms of time-variant TTDs – forward and backward forms – can be distinguished in this framework (Benettin et al., 2015).

Flux tracking models are based on the determinants (i.e., hydrological fluxes/storages) of resulting precipitation partitioning processes. Although these models are often highly conceptualized by, e.g., assuming perfect mixing inside each control volume, they have been proven to be a valuable modeling framework to interpret tracer data and derive catchment-scale TTDs to better characterize the age distribution of water storage and outflow fluxes (Hrachowitz et al., 2013; Benettin et al., 2015; Heße et al., 2017; Remondi et al., 2018). Flux tracking, therefore, helps to estimate TTDs of different water storages and to understand the mixing behaviors of soil water and groundwater (Hrachowitz et al., 2013). If spatially distributed models are used for input, the spatial heterogeneity in TTDs can also be assessed using flux tracking (Heße et al., 2017; Remondi et al., 2018; Kumar et al., 2020).

On the other hand, Lagrangian particle tracking is a physically-based approach that uses the explicit characterization of velocity fields and associated flow lines of the water particles in a heterogeneous subsurface system. Particle tracking can be used to trace the transport pathways of individual water particles under the assumption of dispersive-advective transport or sole advective transport (Eberts et al., 2012; Leray et al., 2016; Davies and Beven, 2012). Such a particle tracking approach is typically linked with three-dimensional, distributed groundwater models that account for unsaturated and saturated groundwater flow and related age estimation (de Rooij et al., 2013; Engdahl and Maxwell, 2015; Yang et al., 2018; Jing et al., 2019). Although being computationally expensive, particle tracking models enable the direct link between TTs and the physical processes. Nevertheless, the particle tracking approach is not immune from certain methodological choices like spatial resolution or discretization of the mesh and geological attributes representing the subsurface system (Sprenger et al., 2019; Maxwell et al., 2019; Jing et al., 2019).

Flux tracking approaches work very well with conceptual hydrological models, i.e., bucket-type models that track water fluxes between different compartments by partitioning precipitation, generating runoff, and reproducing near-surface hydrological variables (e.g., soil moisture and evapotranspiration). Unfortunately, their groundwater characterizations are always implicit and processes are simplified/conceptualized with one or two lumped parameters, resulting in a possibly over-simplified characterization of groundwater flow and transport processes (Fenicia et al., 2006; Stewart et al., 2012). This is mainly due to the fact that the signal near the surface (i.e., discharge or tracer concentration) is insensitive to the variation in groundwater storage. A recent study by Gleeson et al. (2016) demonstrates that only around 6% of total groundwater in the uppermost 2 km over the globe is found to be contributed by contemporary (modern) recharge fluxes, indicating that only a modest portion of the total groundwater storage actively interacts with surface water. Groundwater ages may consequently span a wide range of values (e.g., over 50 years) over a short distance (less than 1.5 m) in the vertical direction (Weissmann et al., 2002). This strong heterogeneity in groundwater ages cannot be explicitly captured by conceptual approaches used with flux tracking, but requires a detailed treatment of subsurface heterogeneity and tracing of water particles through physically-based groundwater models (Jing et al., 2018).

Another important challenge to the TTD characterization is the fact that TTs of water parcels are time-variant and spatially heterogeneous. This transient behavior of TTDs has only been investigated more recently (Botter et al., 2010; Rinaldo et al., 2011; Cornaton, 2012; Harman, 2015; Engdahl, 2017; Kaandorp et al., 2018; Kumar et al., 2020). The temporal variability has been investigated using tracer experiments (Birkel et al., 2011; McMillan et al., 2012; Benettin et al., 2015). The spatial variability in TT behavior, however, cannot be assessed using tracer data in streamflow because this signal is a lumped representation of the whole catchment (Kirchner, 2016). The spatial distribution of water TTs is critical to the assessment of point and nonpoint-source contamination. The spatial variability in TTDs is closely related to the topographical, morphological, and geological properties within the catchment. The inferred mean travel time (MTT) using tracer data is subject to a high aggregation error in heterogeneous catchments (Kirchner, 2016). Some studies unveiled that the shape of TTDs among different catchments can be different (Kaandorp et al., 2018; Abrams and Haitjema, 2018; Remondi et al., 2019). However, the spatial heterogeneity of the grid-scale TTDs parameters (e.g., shape and scale) within a catchment has rarely been investigated.

Although many studies deployed flux tracking methods to estimate catchment-scale TTDs, the characterizations of groundwater storages are often conceptual, indicating that an analytical relationship between the storage and discharge has typically been presumed in a simplified manner (often as the outflow from a linear reservoir). This simplified characterization may lead to severe errors in interpreting tracer data and could essentially underestimate the catchment TTD due to its incapability in “seeing” the old water

(Stewart et al., 2012, 2017). Yet, given the known heterogeneity of subsurface flow patterns, this paucity of spatially explicit representation of the groundwater system restricts the accuracy and reliability of inferred TT. While some studies have begun accounting for spatial heterogeneity in the soil compartment (Heße et al., 2017; Remondi et al., 2018; Kumar et al., 2020), a similar approach to the deeper groundwater system is still missing. Due to this gap, a number of questions remain currently unanswered. For example, what is the explicit role of groundwater in shaping up the travel time distributions (TTDs) of an overall streamflow behavior? In other words, how to disentangle the role of near-surface (soil) and groundwater TTs? How does the spatial heterogeneity of TTDs, resulting from the differences in climate and landscape attributes (e.g., soil and geological features), affect the overall, i.e., catchment-wide TT behavior? And finally, how different are the spatial feature of TTDs corresponding to near-surface and groundwater components? To answer these questions, we comprehensively investigate the spatial and temporal variability in TTDs through the integration of the flux tracking approach with the particle tracking approach. We describe and test the methodology to provide an integrated assessment of the catchment scale, subsurface TTDs accounting for an explicit treatment of the groundwater component using a 3-D groundwater model. We adapted a spatially varying description of transient TTDs through a flux tracking scheme (Hrachowitz et al., 2013; Heße et al., 2017) that accounts for the daily variation in near-surface hydrological processes (e.g., soil moisture, evapotranspiration, fast-flows, groundwater recharge) represented in a distributed surface hydrologic model. The groundwater component is represented through a three-dimensional groundwater model and a particle tracking scheme is used to infer the corresponding groundwater TTs. Both components are interactively linked such that spatial and temporal variability of TTDs can be deduced for each hydrologic compartment at any specified location within a study domain. The proposed modeling framework explicitly accounts for the spatial heterogeneity of climate and landscape attributes including the representing of deep groundwater aquifers. We apply and test the proposed approach in a single densely mapped catchment located in Central Europe.

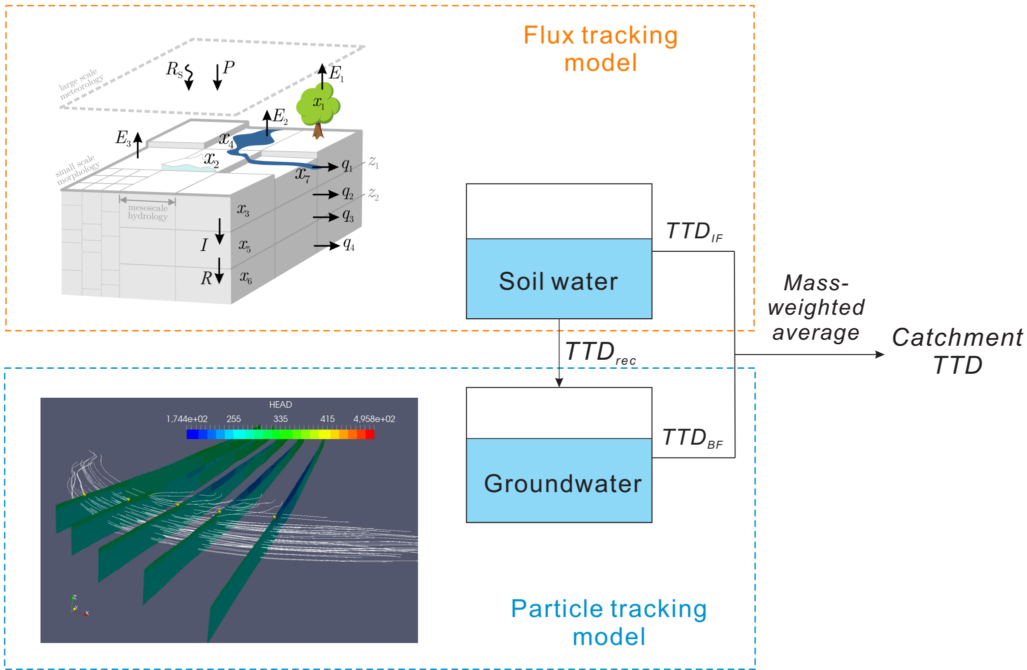

Figure 1: Modeling framework based on the coupled hydrological model mHM-OGS. The modeling framework combines the flux tracking approach with the particle tracking approach to characterize soil-water and groundwater transport processes.

2. Methodology

2.1. Integrated hydrological model

For the numerical modeling of the subsurface water flow, we employ the coupled mHM-OGS model as described by Jing et al. (2018). This model was developed to account for the different challenges faced when modeling near-surface flow, e.g., soil moisture, vs. modeling deeper subsurface flow, i.e, groundwater.

In the coupled mHM-OGS model, the mesoscale Hydrologic Model (mHM; Samaniego et al. (2010); Kumar et al. (2013)) is used to track the surface and near-surface hydrologic fluxes and storages (e.g., root-zone soil moisture, evapotranspiration, infiltration, groundwater recharge). On the other hand, the groundwater model OpenGeoSys (OGS; Kolditz et al. (2012)) is used to simulate the groundwater flow in the deeper aquifers and track the paths of water particles.

mHM is a distributed hydrologic model that employs grid cells as the basic unit, and is capable of simulating various near-surface water fluxes and states. These include interception, surface runoff, evapotranspiration, groundwater recharge, and soil moisture dynamics (Samaniego et al., 2010; Kumar et al., 2013). The root zone has been partitioned into several water storages including the canopy storage (x_1), the snowpack (x_2), the soil moisture content in the root zone (x_3), impounded water in reservoirs or sealed area (x_4), subsurface reservoir (x_5), and groundwater reservoir (x_6). The root-zone is further discretized into three soil layers with the two upper layers end in 0.05 and 0.25 m, and the lowest layer is spatially variable with the depth prescribed based on the soil map (average of around 1.8 m deep; see Zink et al. (2017)). The conceptualization of these water storages can be found in Figure 1, and details of the model parameterizations can be found in Samaniego et al. (2010), Kumar et al. (2013), Livneh et al. (2015), and Heße et al. (2017). The model uses a unique multiscale parameter regionalization (MPR) technique to explicitly incorporate the sub-grid variability of basin physical properties (e.g., terrain, soil and landcover attributes) and facilitates model runs at multiple spatial resolutions (Samaniego et al., 2010; Kumar et al., 2013). mHM can be conditioned and evaluated using various types and sources of data (Rakovec et al., 2016; Zink et al., 2018). The model is available under an open source license and details on model conceptualisation and parameterization can be obtained at `www.ufz.de/mhm`. It has been successfully established for many large-scale applications including to investigate climate change impact assessment studies (Samaniego et al., 2018; Thober et al., 2018).

OGS is a physically-based porous media simulator employing the finite element method to solve subsurface processes (Kolditz et al., 2012). OGS has been successfully applied to cope with a broad range of hydrogeological problems including seawater intrusion, groundwater depletion, and water resources management (Sun et al., 2011; Kalbacher et al., 2012; Jing et al., 2018). OGS explicitly solves the partial differential equations of 3-D unsaturated-saturated groundwater flow.

Two models are linked through a mHM-OGS coupling interface. Through this interface, mHM based spatially distributed recharge and baseflow along stream network are transferred as Neumann boundary conditions in the OGS groundwater model (Jing et al., 2018, 2019). Here we provide a brief overview of the coupling workflow and for more details, please refer to Jing et al. (2018):

1. After calibration, mHM is first run to calculate soil zone fluxes and variables including the recharge and baseflow at the time step t_i.
2. The stepwise routed baseflow, calculated by mHM, is converted into distributed river discharges. This distributed river discharge serves as a Neumann boundary condition in the OGS model.
3. Groundwater recharge estimated by mHM is also interpolated onto the upper surface of OGS mesh, serving as a Neumann boundary condition.
4. OGS model calculates the updated groundwater flow and transport variables at time step t_i, and replaces the original groundwater variables in mHM.
5. The same procedure is repeated at the time step t_{i+1} until the end of simulation.

2.2. Integrated travel time framework

Corresponding to this coupled numerical modeling framework, we deploy different strategies to track the TTs within their respective (soil and groundwater) compartments (see Figure 1). For the water that travels through the soil compartment, we use a flux tracking scheme following Heße et al. (2017). The flux tracking scheme is built upon the bucket-type hydrologic conceptualization, wherein each bucket is presumed to be well-mixed water storage and the water can be stored in the bucket, infiltrated into the deeper bucket, or discharged as runoff or evapotranspiration. The storage-discharge behaviors in each bucket are conditioned by climate forcing and topographical, morphological, and geological properties. This scheme consequently relies on the model results of mHM (see the upper part of the schematic in Figure 1) following Heße et al. (2017). For the water that travels through the aquifer system, we use a particle tracking scheme, namely the Random walk particle tracking (RWPT) algorithm, to track the flow path lines in the heterogeneous aquifer system. RWPT is a Lagrangian particle tracking method assuming that the advection process is deterministic and the dispersion process is stochastic. RWPT has been used to simulate reactive transport processes as well as particle TTs in heterogeneous groundwater systems (Park et al., 2008; Jing et al., 2019). This algorithm is connected to the physically-based groundwater model OGS (see the lower part of the schematic in Figure 1). The integrated TTDs of the whole input water can then be derived through the mass-weighted combination of the component-wise TTDs (Figure 1).

Travel time in the soil compartment

To begin, let us consider the TTD in a control volume CV (e.g., a grid cell). Here, we define interflow as the water flux that infiltrates the soil surface and flows into the stream which typically travels above the groundwater level, and baseflow as the runoff component generated by deep saturated groundwater (Beven, 1989). The hydrological processes in this CV are controlled by an influx J, typically precipitation, as well as several outflux components, namely evapotranspiration ET, Q^{IF} representing the interflow , and R representing the percolation or recharge to the deeper groundwater aquifer. The continuity equation can be given as:

$$\frac{dS}{dt} = J - Q^{IF} - R - ET \tag{1}$$

here, the input flux J contains numerous water particles, each of which enters the system at time t_i and leaves the CV at time t_e as ET, Q^{IF}, or R. For the non-stationary hydrologic system, it is advantageous to distinguish the TT t_T from the residence time t_R. Let us define the TT t_T as the time elapsed by the water particle from entering till exiting the CV: $t_T = t_e - t_i$. Conversely, at a given time t, the residence time t_R is defined as $t_R = t - t_i$.

The forward expression of TTD $p_T(t_T, t_i)$ tracks the TTs of particles injected into the system at a given time t_i. We assume that the soil water storage is well-mixed, wherein the water particles randomly exit as Q^{IF}, R, or ET. Following Botter et al. (2010), the analytical form of the travel time PDF of water parcels exiting as Q^{IF} in a well-mixed storage can be expressed by:

$$p_T^{IF}(t - t_i, t_i) = \frac{Q^{IF}(t)}{S(t)} \frac{e^{-\int_{t_i}^{t} \frac{Q^{IF}+R+ET}{S(x)} dx}}{\theta^{IF}(t_i)}. \tag{2}$$

In this equation, the hydrologic partition function of interflow $\theta^{IF}(t_i)$ is expressed as:

$$\theta^{IF}(t_i) = \int_{t_i}^{\infty} \frac{Q^{IF}(\tau)}{S(\tau)} e^{-\int_{t_i}^{t} \frac{Q^{IF}+R+ET}{S(x)} dx} d\tau. \tag{3}$$

Equation 2 and 3 are forward expressions of travel time PDFs for water particles discharged as interflow. Similarly, PDFs for water particles recharged to the deep groundwater aquifers $p_T^R(t-t_i, t_i)$ can also be expressed using Equation 2 and 3 by swapping Q^{IF} with R.

Travel time in the groundwater compartment

Water particles that recharged into the deeper groundwater aquifers are traced using RWPT in an explicit three-dimensional groundwater model. For such a system, let $p_T^{GW}(t)$ represent the TTD of water particles passing through groundwater aquifers estimated by the RWPT method. Then the TTD of water particles from their entrance to the subsurface system (through recharge) until their discharge as baseflow can be expressed using the following convolution integral:

$$p_T^{BF}(t-t_i,t_i) = \int_{t_i}^{\infty} p_T^{R}(\tau-t_i,t_i)p_T^{GW}(t-\tau+t_i)d\tau. \tag{4}$$

This convolution represents the fact that the TT of any water parcel leaving as baseflow can be considered as a the sum of two random variables: the TT for passing through the soil compartment and the TT for passing through the groundwater compartment (see schematic in Figure 1). Once the TTs for water parcels leaving as interflow and baseflow are determined, the integrated TT for water parcels leaving the entire subsurface can be computed.

Integrated travel time in the subsurface

The catchment-wide, subsurface TTD $p_T^{SS}(t-t_i,t_i)$ can now be calculated by the mass-weighted average of $p_T^{IF}(t-t_i,t_i)$ and $p_T^{BF}(t-t_i,t_i)$. Note that for the grid cell-based hydrologic model, the catchment TTD can be calculated by mass-weighted averaging the TTD of each grid cell over the whole catchment.

$$p_T^{SS}(t-t_i,t_i) = \theta^{IF}(t_i)p_T^{IF}(t-t_i,t_i) + (1-\theta^{IF}(t_i))p_T^{BF}(t-t_i,t_i). \tag{5}$$

In the above described way the catchment TTD can be realized by linking flux tracking in the soil zone and particle tracking in the groundwater storage (Figure 1).

Using the above modeling framework, we can analyse the spatio-temporal behaviour of the resulting TTDs. Furthermore, we also characterize the marginal (quasi-stationary) behaviour of TTDs through a time averaging approach (Heße et al., 2017).

Summary statistics

We use several summary statistics to characterize and compare the shape and scale of TTDs in different hydrological compartments. These include the mean travel time (MTT), the median TT, the standard deviation (SD), the coefficient of variation (CV), and the interquartile range. Besides, for the parametric form of mean TTDs, we choose the two-parameter Gamma distribution. This parametric distribution can account for the nonlinear behavior and the heterogeneity of the reservoir (Kirchner et al., 2000; Hrachowitz et al., 2010). The gamma distribution has two parameters – a shape factor α and a scale factor β; and its PDFs can be expressed as:

$$p(t) = \frac{t^{(\alpha-1)}}{\beta^{\alpha}\Gamma(\alpha)} e^{-t/\beta} = \frac{t^{(\alpha-1)}}{(\bar{t}/\alpha)^{\alpha}\Gamma(\alpha)} e^{-\alpha t/\bar{t}} \tag{6}$$

where t is the travel time, and $\bar{t} = \alpha\beta$ is the mean travel time.

2.3. Study area

To exemplify the use of this integrated travel time framework, we applied it to the Nägelstedt catchment, located in central Germany (Figure 2). The study area is a mesoscale headwater catchment of the Unstrut river catchment, with an area of approximately 850 km^2. The terrain elevation in the study area ranges from 166 m to 516 m above mean sea level. The climate is classified as warm temperate, fully humid, and warm summer – a Cfb type according to the Köppen-Geiger method (Kottek et al., 2006). The mean annual precipitation is around 660 mm, and the mean annual temperature is around 8.3 degrees Celsius. As shown in Figure 2, four 1 $\times$ 1 km^2 grid cells are selected as samples for tracing water travel times. These four grid cells are selected to cover both the groundwater recharge areas at highlands (C2 and C4) and drainage areas (C1 and C3). The locations of these selected cells with varying geographical characteristics are depicted in Figure 2. Specifically, C1 is a grid cell at a lowland close to the discharge point. C2 represents the grid cell in the western mountainous area close to the left tributary. C3 represents the point at the central lowland near the mainstream, and C4 represent the eastern mountainous area close to the right tributary.

The study area is intensively used for agricultural purposes. Around 78% of the total land in this area has been classified as arable land (Wechsung et al., 2008). Around 17% of the land is marked as forests, while the remaining 5% is regarded as urban areas (Heße et al., 2017) (Figure 2). Groundwater

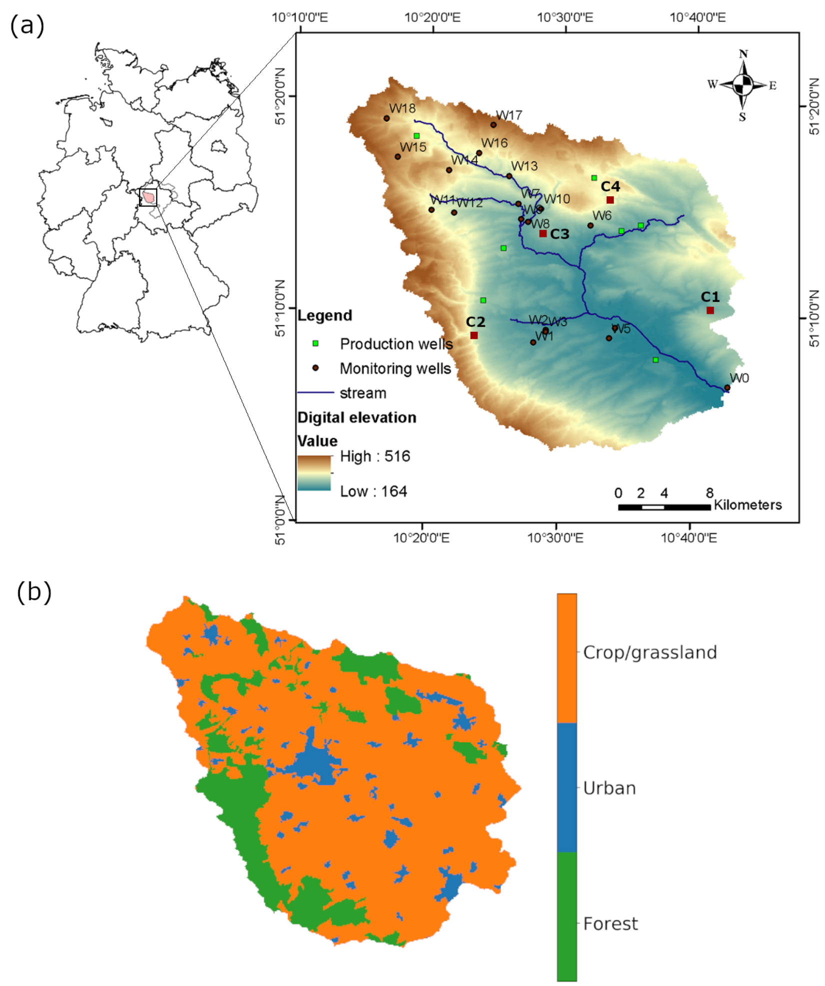

Figure 2: Study area of the Nägelstedt catchment. Panel (a) is the map of the Nägelstedt catchment, which also shows the locations of four sampled 1 km grid cells, whereas panel (b) shows the detailed land-use type in the area. Four cells represent four topographic types: C1 – lowland close to the catchment outlet, C2 – western highland close to the left tributary, C3 – central lowland near the mainstream, C4 – eastern highland.

plays a critical role in supplying public water in this area (Wechsung et al., 2008).

The main geological unit in Nägelstedt catchment is Muschelkalk. Muschelkalk is mainly composed of marine sediments (Figure 3). It can be further divided into three sub-units, which are Upper Muschelkalk (mo), Middle Muschelkalk (mm), and Lower Muschelkalk (mu; Figure 3). Besides, the Keuper sediments overlying the Muschelkalk form an aquifer-aquitard system in the central floodplain. The Keuper can be divided into Middle Keuper (km) and Lower Keuper (ku), wherein the Lower Keuper has a high content of grey clay and may form an aquitard (Figure 3).

This catchment is dominated by agriculture land with a high risk of groundwater contamination due to intensive agricultural activities (Wechsung et al., 2008). The fate of input water is of high relevance with groundwater quantity and resilience. Additionally, this area is also a target area of the AquaDiva project (`http://www.aquadiva.uni-jena.de/`), which aims to cope with environmental problems by multi-disciplinary investigations of biogeochemical processes in the Hainich critical zone observatory (Küsel et al., 2016; Kohlhepp et al., 2017).

2.4. Model setup, calibration, and evaluation

The mHM and OGS models were established and calibrated for this catchment using the framework described in Jing et al. (2018) and Jing et al. (2019). The distributed mHM simulations were established at a daily time step over 60 years (1955 – 2004) and with a spatial resolution of 500 m $\times$ 500 m. The climate forcings driving the mHM model (e.g., atmospheric temperature and precipitation) are based on the observations from the German Meteorological Service (DWD). Other data for the mHM model setup include the DEM data, the land-cover data, the soil-type data, the hydrogeological data, and the discharge data (Heße et al., 2017; Jing et al., 2018). A detailed evaluation of the mHM model including simulations of near-surface fluxes such as runoff, evapotranspiration, and groundwater recharge has been presented in several past studies (Zink et al., 2017; Heße et al., 2017; Jing et al., 2018).

For the groundwater model, we used a three-dimensional mesh based on a Digital Elevation Model (DEM) with a spatial resolution of 25 m combined with information on the geological zonation. We established a stratigraphic model based on the geological data from the Thuringian State Office for the Environment and Geology (TLUG). Based on this, we used a mesh with a

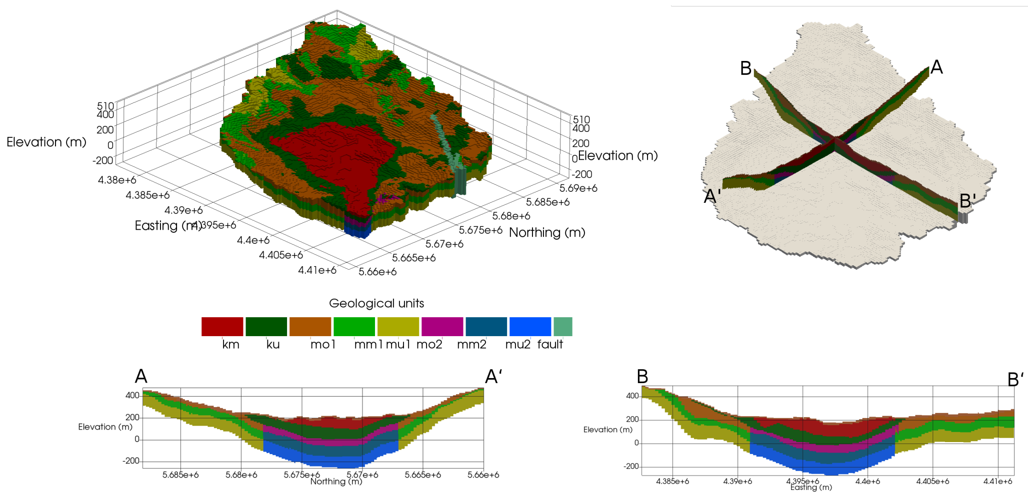

Figure 3: Geological zonation of the Nägelstedt catchment. The full names of abbreviations are: km – Middle Keuper, ku – Lower Keuper, mo – Upper Muschelkalk, mm – Middle Muschelkalk, and mu – Lower Muschelkalk.

Table 1: Bounds and calibrated values of zoned hydraulic conductivities of aquifers.

Geological units	Hydraulic conductivity (m/s)		
	Lower limit	Upper limit	Calibrated value
km	1.0×10^{-6}	5.5×10^{-3}	1.145×10^{-5}
ku	1.0×10^{-7}	3.4×10^{-4}	3.714×10^{-6}
mo1	8.0×10^{-8}	2.0×10^{-3}	2.936×10^{-5}
mm1	1.0×10^{-7}	9.0×10^{-4}	2.184×10^{-5}
mu1	5.0×10^{-9}	2.0×10^{-4}	2.258×10^{-6}
mo2	1.0×10^{-8}	5.0×10^{-4}	2.936×10^{-6}
mm2	3.0×10^{-8}	9.0×10^{-5}	2.184×10^{-6}
mu2	5.0×10^{-10}	2.0×10^{-5}	2.258×10^{-7}

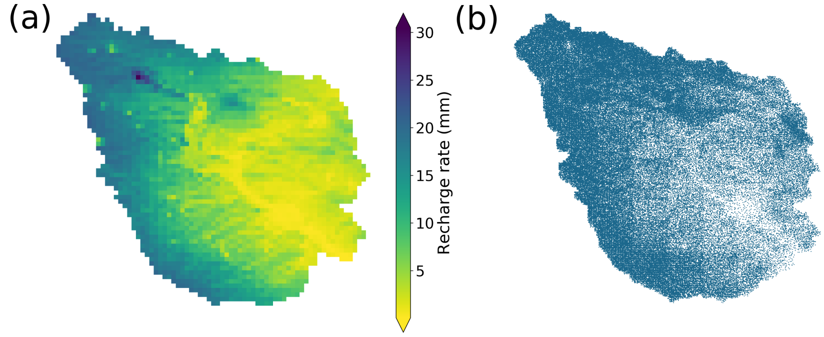

Figure 4: Long-term averaged monthly groundwater recharge over the simulation period (a) and the corresponding spatial organization of released $100,000$ particles for the particle tracking (b).

spatial resolution of 250 m $\times$ 250 m $\times$ 10 m (in x, y, and z directions, respectively (Fischer et al., 2015). Specifically, the less permeable Muschelkalk zones underlying the Keuper formation (mo2, mm2, and mu2) are distinguished from the more permeable Muschelkalk zones (mo1, mm1, and mu1; see Table 1). This three-dimensional mesh is shown in Figure 3.

Moreover, we also account for the uncertainty in prescribing the hydraulic conductivity values in different geological formations, and their contribution to the simulated groundwater and resulting travel times. Specifically, we generate an ensemble of hydraulic conductivity fields using the null-space Monte Carlo (NSMC) approach (Tonkin and Doherty, 2009). The range and distribution of parameters for this uncertainty analysis can be found in Appendix Figure B.14.

Here, we assume steady-state transport processes in the deep groundwater aquifers. This assumption is only limited to the OGS model. This assumption is justified due to fluctuations in recharge rates having only a minor influence on groundwater TTDs (Benettin et al., 2015; Engdahl, 2017; Jing et al., 2019) given the large storage of groundwater systems. We then assigned a no-flow boundary condition at the bottom and outer perimeter of the mesh, whereas a fixed head boundary condition was assigned on the stream beds of the perennial rivers (the river network can be found in Figure 2). To track the flow paths of water parcels, we released a large number of particles ($100,000$ particles) at the top surface of the mesh. The spatial distribution of these particles was arranged to meet the spatial distribution of the mean recharge fields (Figure 4).

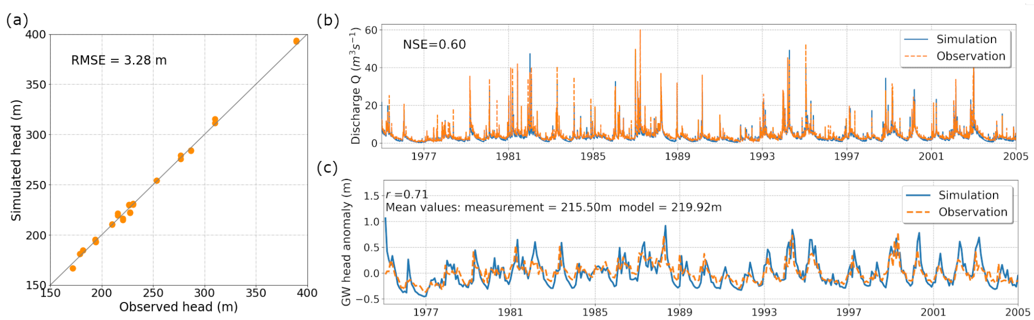

Figure 5: Calibration and evaluation of the coupled mHM-OGS model using the long-term averaged groundwater levels (a), discharge (b), and the time series of groundwater levels at W17 (c). The simulated time series of discharge is 30-year long and at a daily step. The groundwater levels are monitored at 18 monitoring wells (locations of wells are shown in Figure 2) and simulated at a monthly time step.

In the calibration phase, the model satisfactorily computed the daily discharge at the catchment outlet over a 30-year period. The calibrated model demonstrated good capability in reproducing high-frequency discharge (Figure 5). The skill score based on Nash-Sutcliffe Efficiency (NSE) is 0.60, which is satisfactory considering the 30-year simulation period and daily resolution. Simulated dynamics of evapotranspiration and groundwater recharge were also evaluated and validated by the observation at eddy-covariance stations and the Hydrological Atlas of Germany (Heße et al., 2017; Zink et al., 2017). These results confirmed the reliability and accuracy of mHM in capturing the soil-zone water dynamics. We then calibrated the OGS groundwater model against the observed groundwater levels (1955 – 2004) at 18 spatially-distributed monitoring wells (Jing et al., 2018, 2019). Hydrogeological parameters of the calibrated groundwater model are shown in Table 1. The OGS model was also capable to reproduce the pattern of groundwater circulation in the deep aquifers (Figure 5). To confirm the accuracy and reliability of the mHM-OGS model in simulating the groundwater dynamics, we evaluate the modeled groundwater using observations of multiple distributed monitoring wells, wherein 30-year time series of observed groundwater levels are available. The evaluation results are shown in Figure 5 and Figure A.13. In this evaluation phase, the model also satisfactorily simulated the response of groundwater levels to climate forcing (Figure 5 and Appendix Figure A.13). The calibrated model was able to adequately characterize the observed trend and magnitude of monthly groundwater level fluctuations across the observation wells (Figure 5 and Appendix Figure A.13). This is demonstrated by Pearson correlation coefficient (r) values of 0.71, 0.82, 0.48, 0.81, and 0.70 for five monitoring wells, respectively. Based on this successful establishment and evaluation exercise, the coupled mHM-OGS model was used to track the movements and TTs of water parcels across the whole catchment.

3. Results

In the following, we show the application of this integrated modeling framework for a single case study, namely the Nägelstedt catchment. We track the TTs of water inputs from January 1955 to December 1974 because the 60-year data (1955–2004) of the precipitation and discharge enable the tracing of water influxes in this period for the following 30 years (1974–2004). Specifically, we show the spatial variability in TTDs associated with different spatial scales (grid scale and regional scale), the temporal variability of catchment TTD, the contribution of groundwater to the catchment TTD, and the sensitivity of component-wise TTD to the climate forcing.

3.1. Sensitivity of groundwater TTDs to spatial scale and topography

Figure 6 shows the groundwater TTDs for the catchment and for four selected 1×1 km^2 local grid cells (C1, C2, C3, and C4). The analysis results presented here correspond to the derived TTs for water particles from their entrance to their exit from the deep aquifers. We also fit the gamma distribution against the simulated catchment-scale groundwater TTD to show its preference for discharging young/old water. The catchment-scale groundwater TTD shows a preference for discharging younger water with a α value of 0.71. The parameter α of the gamma distribution characterizes the shape of TTDs. A α value less than 1 indicates a strong initial peak and a long tail. However, the grid-scale groundwater TTDs exhibit a strong spatial variability in both shape and scale. Simulated groundwater TTDs in C1, C2, C3, and C4 have diverse shapes and scales, which also deviate from the catchment groundwater TTD. This is attributed to their different hydrogeological conditions and the resulting different layout of the flow pathways (e.g., the occurrence of preferential pathways in some cells due to the more permeable geological formation). Meanwhile, the mean travel times (MTTs) of groundwater in these cells vary widely, ranging from 70.4 years for C4 to 115.2 years for C1. This pronounced spatial variability in the MTTs shows the distinct behavior of flow paths and velocities of water particles for different

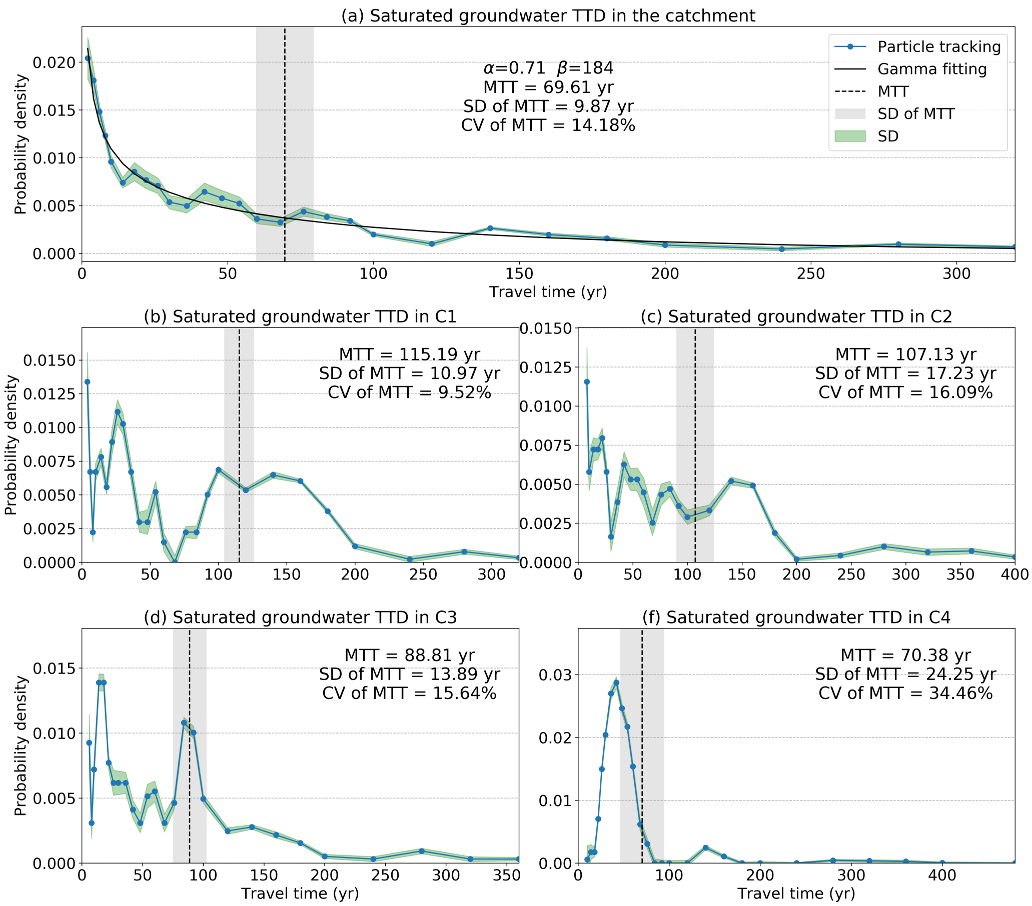

Figure 6: Groundwater TTDs in the whole catchment (a) and in four sampled 1 × 1 km^2 cells (b-f). The green shading area shows the standard deviation (SD) of simulated TTD using an ensemble of hydraulic conductivity fields. The grey shading area shows the SD of MTT using an ensemble of hydraulic conductivity fields. The SD and coefficient of variation (CV) of MTT are also shown in this figure.

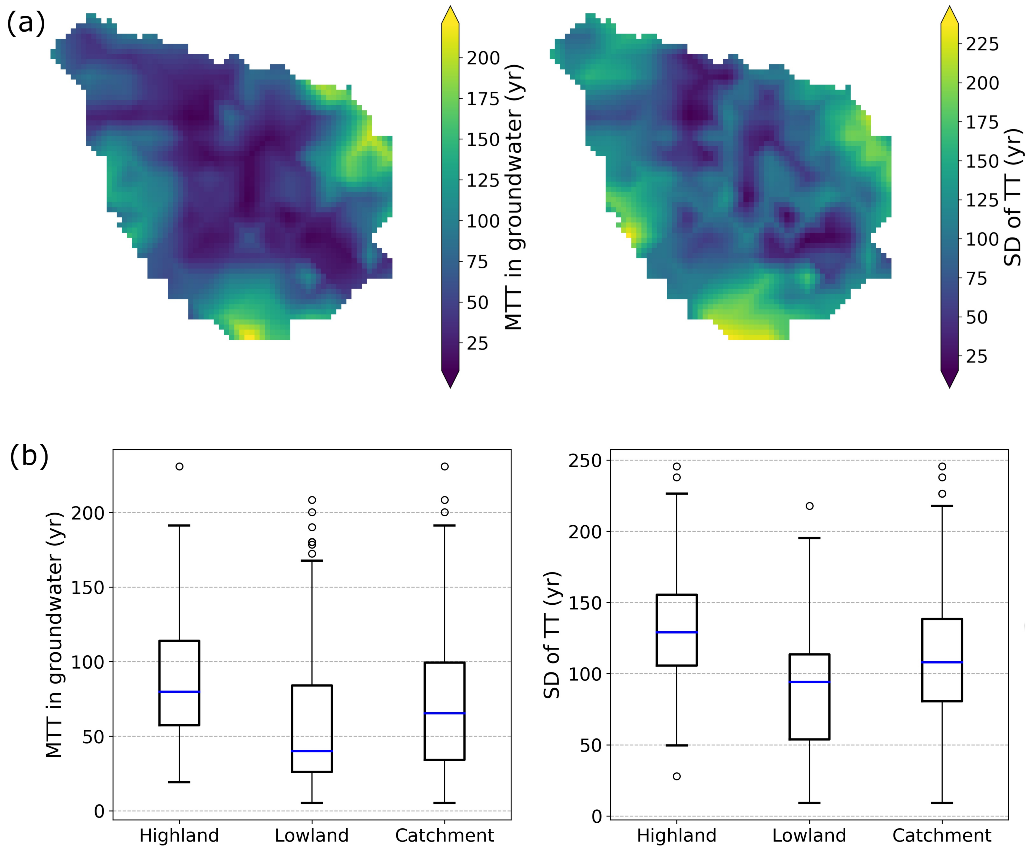

Figure 7: Spatial pattern of the groundwater MTT, SD of TT, and CV of TT for 1×1 km^2 grid cells. Panel (a) shows the overall spatial distribution, whereas panel (b) categorize them by lowland, highland, and the whole catchment.

areas. The parameter uncertainty in hydraulic conductivity propagates to the simulated groundwater TTD, which is demonstrated by the coefficient of variation (CV) of the catchment-scale groundwater MTT (14.2%).

The spatial distributions of the mean and standard deviation of groundwater TT (MTT and SD) in distributed 1×1 km^2 grid cells over the whole catchment are shown in Figure 7. Specifically, we category the grid cells into central lowland and surrounding highland according to topography. We find a strong spatial heterogeneity in MTT of grid-scale groundwater TTDs. Noticeably, the volume-averaged TTD in the surrounding highland is about twice as large as that in central lowland. The groundwater MTT ranges from years to decades for lowland, whereas these values lie in the decadal to

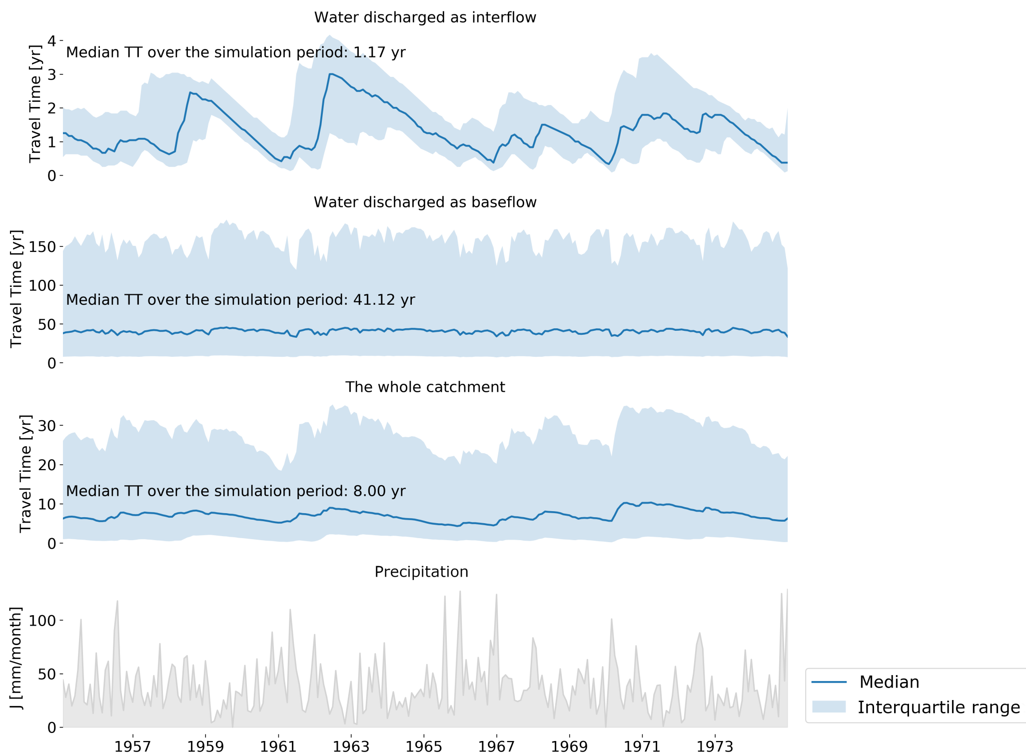

Figure 8: Time series of the simulated catchment TTs from 1955 to 1974. First three panels show the time series of medians (solid lines) and interquartile ranges (shading areas) of TTs. The fourth panel shows the time series of the monthly precipitation rate.

centurial scale for the outer highlands. This is mainly attributed to the relatively sparse stream network and the lower hydraulic conductivity of main geological formations in the highland area. The SD of TTs also shows similar spatial structure – SD is generally lower in central lowland around the vicinity of the stream network and higher at highland far away from streams. These two summary statistics provide not much information on the shape of grid-scale groundwater TTDs, but we can expect a large variability in them based on the distinct shape of four sampled TTDs (Figure 6).

3.2. Climate control on water travel times

Tracking historical trajectories of the TTs over a long period of precipitation events helps us to understand the relationship between time-variant TTs and the resulting hydrologic controls. Figure 8 shows the time series of

TTs and the corresponding monthly precipitation rates over the span of 20 years (1955-1974). Figure 8 shows a large temporal variation in the median TTs of soil-water interflows, which closely follow the temporal dynamics of precipitation.

In general, higher precipitation rates result in a shorter TT of soil water, a result well known from the literature. We can also observe a significant seasonality in soil-water TT, which is largely attributed to the seasonal variation in precipitation and evapotranspiration (Figure 8). Conversely, the temporal fluctuations in precipitation have a minor effect on the TT of groundwater. There is no seasonal pattern in the groundwater TTs (see the second panel in Figure 8). The integrated TT of the whole catchment has an intermediate temporal variability, which is attributed to the fact that the catchment TTD is a weighted average between the soil zone TTD and the groundwater TTD. The median TTs over the 20-year simulation period are around 1.2, 41, and 8 years for the soil water interflow, groundwater baseflow, and the total streamflow, respectively. The groundwater TTs show the largest interquartile range, indicating the large time scale (e.g., decade) of the groundwater transport processes. The interquartile range is also strongly inversely related to precipitation such that low precipitation causes a larger interquartile range of water TTs. These simulation results through the integrated modeling framework reveal the contrasting TT characteristics of the different hydrological compartments.

We use the modeling framework to understand the effect of climate forcing on the varying behavior of water transport and mixing in different hydrologic compartments. Specifically, we evaluate the characteristics and response of the hydrologic partition function (Equation 3) and the resulting median TTs of different hydrological compartments to varying hydroclimatic conditions (Figure 9).

In a scatter plot shown in Figure 9, the individual points represent the monthly-averaged values for 40 years from 1955-1995. We separated the 40 years (time-period) into wet and dry years depending on the deviation from the average annual effective precipitation rate. Effective precipitation is defined as the precipitation that is not evapotranspired and eventually discharges into streams. The hydrologic partition function for water discharged as interflow (θ^{IF}) is positively related to higher effective precipitation, indicating the key part of hydroclimatic forcing in partitioning the water budget and generating quick interflows. The θ^{IF} values in many years deviate from the (fitted) regression line (Figure 9). This is because θ^{IF} is a function of

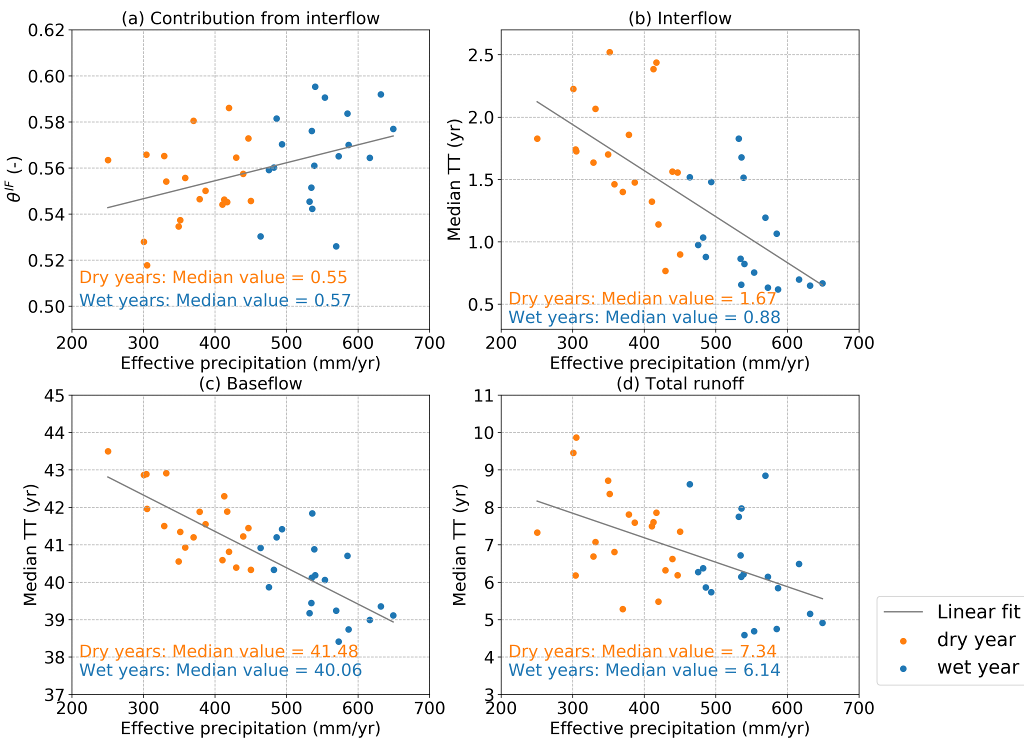

Figure 9: Dependence of water TTs on time-variant climate forcing (effective precipitation). Precipitation controls the hydrologic partition function θ^{IF}, i.e., the contribution of interflow to the overall TTDs (panel a). The dependence of median travel time in interflow (panel b), baseflow (panel c), and total runoff (panel d) on effective precipitation are also shown in different panels.

all precipitation events after water parcels enters into the catchment rather than the precipitation events of a given year.

MTTs are negatively correlated with the effective precipitation in the soil zone, groundwater aquifer, and the whole catchment, although with different degrees of absolute values. The MTTs in the soil zone are more sensitive to the climate forcing with the MTTs in dry years being on average two times higher than the values observed in wet years. The dependency of MTTs on hydro-climatic conditions for baseflow is not as pronounced as that for interflow. The MTTs for the whole catchment show the moderate response with values in the wet years being on average 20% lower than those observed during dry years.

3.3. Contribution of groundwater to catchment TTD

The numerical framework described here allows for the investigation of space/time behavior of TTDs in different hydrologic compartments and their contribution to overall TTD. Here we explicitly examine the role of component-wise TTDs and their relationship to the integrated catchment signal. Specifically, we show how the parameter uncertainty in different hydrologic components affects the predictive capability of the integrated TTD.

Figure 10 shows the probability density functions (PDFs) for water TTs discharged as interflow, baseflow, and the total runoff over the whole catchment from 1955 to 1974. The catchment TTD exhibits a power-law behavior with a significant long tail (Figure 10. This indicates that the catchment discharge is comprised of water parcels with a wide range of travel times. The mean TT of water particles discharged as interflow ($\mathrm{MTT_{IF}}$) is approximately 1.93 years. Conversely, the mean TT of water particles discharged as baseflow ($\mathrm{MTT_{BF}}$) is 74.16 years. Based on the hydrologic partition function, the mean TT for the whole catchment ($\mathrm{MTT_{Q}}$) is 37.50 years. It is worth noting that the estimated MTT is much larger than the corresponding median TT in every hydrological compartment, which emphasizes the asymmetric long-tail behavior of the TTDs (Figure 8 and Figure 10). We could also observe a narrower shading width towards the higher tails of the TTDs, indicating a decreasing (temporal) variance in the probability function with increasing TT. There is also a contrasting shape (width) between the TTDs of the two hydrologic compartments – with a larger temporal variability for the soil-water TTs than that of the groundwater TTs. We attribute this to the relatively more dynamic fluxes and storage volumes in the shallow soil

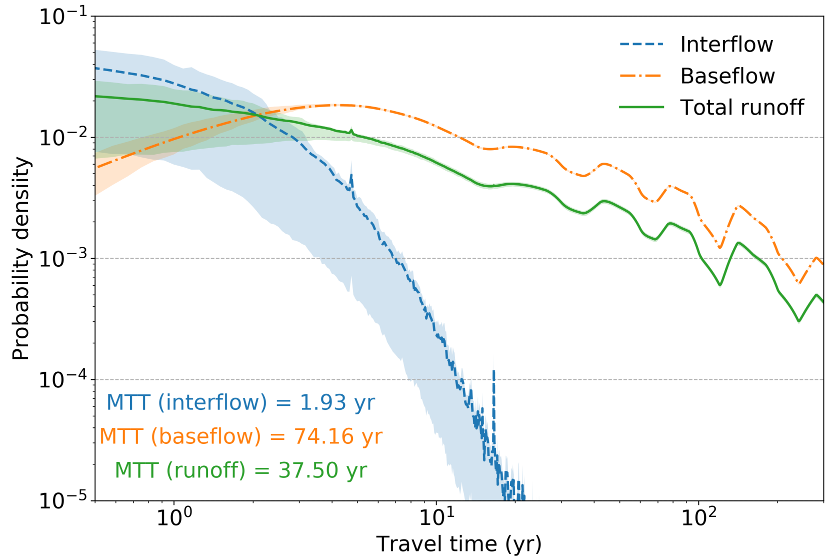

Figure 10: PDFs of catchment-scale TTD of water discharged as interflow, baseflow, and total runoff from 1955 to 1974. Shaded area denotes the interquartile range of all individual monthly TTDs over this period.

zone compared to those in the deep groundwater aquifer. This also reveals the damping effect of the catchment to the input signal (e.g., precipitation).

Figure 11 shows the simulation results of the grid-scale TTDs in four 1×1 km^2 grid cells through the mass-weighted average of the TTDs of interflow and the TTDs of baseflow. A remarkable difference in the scales of the interflow TTs and baseflow TTs can be observed across the four analyzed locations. The MTTs of water discharged as interflow are approximately 2 years for all four cells, whereas the $\mathrm{MTT_{BF}}$ values vary over a wide range (63.18 – 96.78 years). As a mass-weighted average between the above two TTDs, the integrated mean TTs of the total runoff range from 38.43 – 61.39 years. The shapes of the integrated TTDs are irregular due to the distinct shapes and time scales of soil-water TTDs and groundwater TTDs. The shapes of the integrated TTDs are dominated by the soil-water for an early period, e.g., TTs less than 1 year, and thereafter by the groundwater for the tails of the distribution (Figure 11). We can also observe a multi-modal shape of the overall TTD for the C4 cell, which is mainly controlled by the complex aquifer geometry and stratigraphy. Overall TTDs in C1, C2, and C3 present similar power-law shape and fractal behaviors. The MTTs of

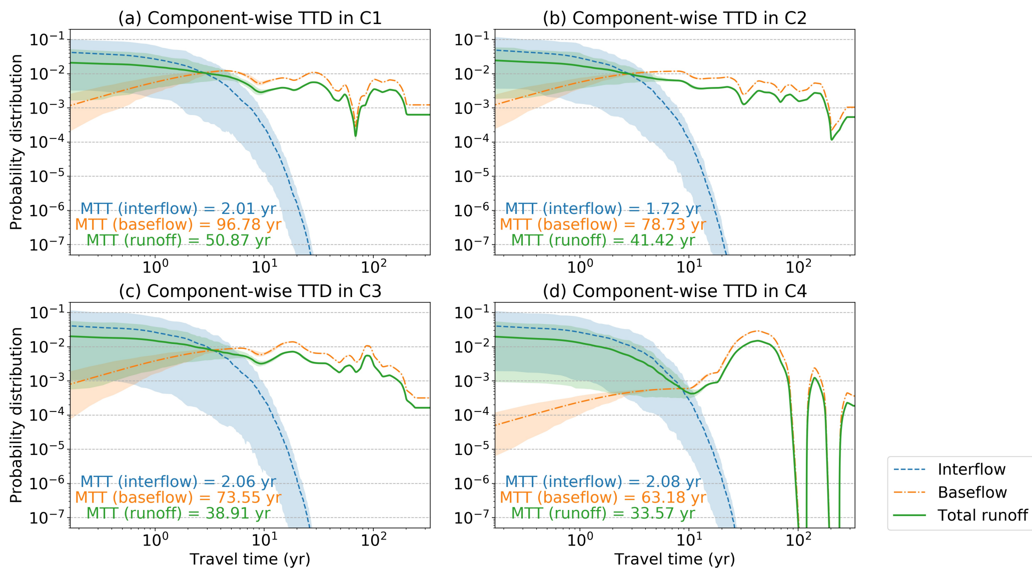

Figure 11: Grid-scale TTDs of input water that eventually discharged as interflow, baseflow, and total runoff in four sampled 1 × 1 km^2 grid cells.

overall discharge flux show a strong spatial heterogeneity, which is largely due to the heterogeneous MTTs in baseflow. Moreover, the decadal scale of MTT of total runoff can be attributed to the long tails of baseflow TTD. This signifies the importance of appropriate characterization of deep groundwater such that it strongly controls the scale of overall MTTs.

3.4. Predictive uncertainty in catchment TTD

We further study the influence of uncertainties in different hydrological compartments and their contributions to the total uncertainty in streamflow signal. The simulation results in Subsection 3.1 already shows that the parameter uncertainty in aquifer hydraulic properties results in a 14.18% variation in simulated groundwater MTT. Accordingly, we investigate how this degree of variation in groundwater affects the predicted overall MTT in streamflow. We also set up a reference scenario wherein the same degree of variation in soil water MTT is considered, and compare the predictive uncertainty in overall MTT in these two scenarios. We then calculate the induced variation in median TT of the catchment from the same degree of variation in soil zone and groundwater.

Figure 12 clearly shows the contrasting degree of predictive uncertainty in

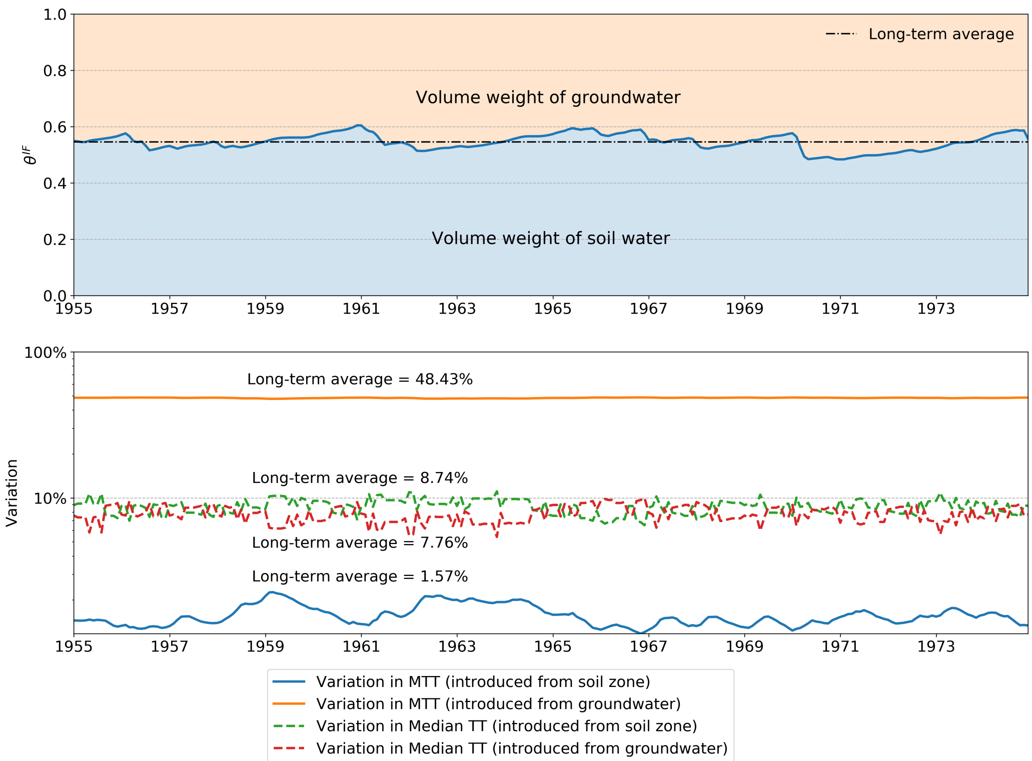

Figure 12: Uncertainty in simulated MTT and Median TT introduced from different hydrological compartments from 1955 to 1974. The upper panel shows the time-dependent hydrologic partition function θ^{IF}. The lower panel shows the variation in catchment MTT and Median TT introduced from the variation in groundwater and soil water, respectively.

these two scenarios. Note that the volume contribution of soil zone and deep groundwater is computed using the hydrologic partition function θ. We find that the contribution from the soil zone is about 56%. A 14.2% variation in groundwater MTT leads to an around 48.4% variation in catchment MTT, whereas the same variation in soil water MTT only results in an around 1.6% variation in catchment MTT. However, the same level of variation in soil zone and groundwater only leads to 8.7% and 7.8% variations in catchment-scale median TT. This indicates that although the volume contributions from soil water and groundwater to the streamflow are almost equal, the sensitivities of catchment MTT to them are distinct. In the study area where baseflow from deep groundwater substantially makes up a large portion of streamflow, catchment MTT is extremely sensitive to variation in groundwater and not sensitive to that in soil water. Although quick interflow from soil zone constitutes about 56% of the total volume of streamflow, their TTs appear to have a minor influence on the overall MTT. Alternatively speaking, MTT is not representative of the transport processes in the soil zone, even if the volume of interflow constitutes more than half of the total volume of streamflow. The sensitivities of catchment-scale median TTs to soil zone and groundwater seem to be consistent with the volume weights of these two components, indicating that the median TT is more robust in terms of representing the overall behavior of water transport processes relative to the MTT.

4. Discussion

This study introduces a novel modeling framework that couples the flux tracking approach and the particle tracking approach to achieve a full, spatially-explicit description of subsurface TTDs. We use this modeling framework to investigate the spatio-temporal behaviors of TTDs in different compartments of the subsurface water cycle in the Nägelstedt catchment. Although the simulations in this study are particular to the study area, the method used here is applicable to other regional catchment. The numerical simulation results have important implications for understanding the transient and spatially heterogeneous TTs in subsurface systems.

4.1. Spatial variability in TTDs and its dependence on topography and aquifer structure

The proposed modeling approach explicitly characterizes the spatial variability in component-wise water TTDs across scales (from grid scale to catchment scale). Therefore, it facilitates the study of topographic and geologic controls on catchment TTDs. Since we could observe a significant influence of the subsurface hydraulic heterogeneity on the shapes of grid-scale TTDs, it follows that the explicit characterization of subsurface heterogeneity is a nontrivial element to a comprehensive characterization of TTDs (Figure 11). This influence can be attributed to the complex spatial organization of flow pathlines within the aquifer system, resulting from a said pattern of stratigraphy. These findings are in-line with the ones described by Danesh-Yazdi et al. (2018) and Kaandorp et al. (2018), who also report strong variability in the shapes of TTDs either using different realizations of hydraulic conductivity fields or in different catchments. We also observe different patterns of groundwater TTD for central lowland and surrounding highland, which is likely related to the distance to the groundwater discharge zone and the underlying subsurface structure. A similarly strong dependence of TTD on topography has been reported in other real-world catchments (Cardenas, 2007; Remondi et al., 2019).

The contrasting shapes and scales of groundwater TTDs in different investigated cells (see Figure 7 and Figure 8) highlight the key role of subsurface heterogeneity in controlling the flow paths and TTs of water parcels. This effect is unveiled by direct simulation of the pathways and velocities of a large number of released particle tracers using the RWPT algorithm. Investigating the relationship between the properties of the aquifer system and the behavior of groundwater TTDs revealed a number of relevant relationships. The strong spatial heterogeneity in the shapes of grid-scale groundwater TTD is mainly introduced by the stratigraphical structure of the aquifer system and the zoned hydraulic conductivity distribution prevailed across the study area. The grid-scale MTT appears to be closely related to the distance of the corresponding grid cell to the stream network. These findings are in-line with Fiori and Russo (2008) and Ameli et al. (2016), wherein they also found a strong dependence of TTD on the vertical pattern of hydraulic properties.

The aforementioned strong spatial variability of TTs has greater implications for the assessment of nonpoint-source agricultural contamination. The long tail and fractal behavior of catchment TTD imply a high risk of legacy contamination in the Nägelstedt catchment wherein agricultural activities are extremely intensive (Wechsung et al., 2008). The proposed mHM-OGS modeling framework could therefore be a valuable tool in revealing the intrinsic mechanism of the legacy nitrogen in streamflow, which has been frequently reported in many catchments across Germany and the globe (Mueller et al., 2016; Van Meter et al., 2017, 2018).

4.2. Temporal variability in catchment TTD conditioned by precipitation

The second contribution of this study is on the time-varying impact of soil water and groundwater to the integrated TTDs. This finding is crucial to the understanding and prediction of the fate and the TTs of nonpoint-source input solute such as agricultural contaminants. In general, we observe a decrease in variability for longer times (see Figure 10 and Figure 11). This can be attributed to the different sensitivities of the shallow soil storage and the deeper groundwater aquifer to the climate forcing. The shallow storage is highly dynamic due to being subjected to the highly-dynamic input of precipitation, its small storage volume (compared to the deeper groundwater system), the varying land-use type, and the impact of evapotranspiration (Benettin et al., 2015). Conversely, the deeper groundwater aquifer system has a large storage volume and no (apparent) direct connections with the atmosphere leading to the overall less dynamic input forcing in the form of groundwater recharge (Jing et al., 2019; Heße et al., 2017). The hydroclimatic conditions also control the contribution from different hydrological compartments to the overall TTD. The median travel time in dry years is expected to be larger than that in wet years, implying that transport and mixing characteristics of the catchment will be altered by the changing climatic conditions. This is attributed to the fact that higher precipitation essentially increases the hydraulic potential difference in both soil and groundwater, and thus activates shallow flow pathlines (Kaandorp et al., 2018; Remondi et al., 2019). These kinds of response behaviors (TTs vs. climate forcings) noticed here are in-line with those of Remondi et al. (2018) and Jing et al. (2019), wherein they also found a strong dependence of catchment TTs on hydroclimatic forcing conditions.

4.3. Contribution of different hydrological compartments to catchment TTD

This study provides insights into the constitution of catchment TTD of different hydrological compartments. Compared with the partition of the hydrograph, the partition of water mass in streamflow suffers from a wider range of uncertainty, which is mainly attributed to the difficulty in quantifying contribution from slow baseflow component (Stewart et al., 2012). Tracer-based analysis (e.g., interpretation of Tritium data using lumped parameter model) is a common approach used for this purpose, but it also suffers from many sources of error such as the aggregation error (Kirchner, 2016; Stewart et al., 2017). The application in the Nägelstedt catchment is built on a 60 years' of the daily hydroclimatic forcing data and a 3-D stratigraphic aquifer model, therefore explicitly accounts for the spatial and temporal heterogeneity that facilitates the forward-type of particle tracking. The partitioning of contributions from different hydrological compartments is achieved through the hydrologic partition function θ, which explicitly tracks all precipitation events after the entrance of water parcels to the catchment. Several recent studies have also demonstrated the advantages of forward simulation of travel times in explicitly accounting for the constitution of catchment TTD (Koh et al., 2018; Eberts et al., 2012).

4.4. Uncertainty and robustness of MTT in describing catchment transport processes

The catchment TTD exhibits a power-law behavior with a high probability at an early stage and a long tail (Figure 10 and Figure 11). This tailing behavior is also revealed by the strong deviation from MTT (37.50 years) to median TT (8 years) of the catchment. The decadal scale of catchment MTT has also been reported in several tritium-based studies, although the catchment properties may vary greatly from this study (Cartwright and Morgenstern, 2015; Stewart et al., 2017). The power-law behavior also exhibit the uncertainty propagating from parameters (varying hydraulic conductivity values) to groundwater simulations and the resulting TTDs. In the study area, the same degrees of uncertainty in soil zone and groundwater can lead to distinct scales of predictive uncertainty in MTT, although the volume contributions from two components to streamflow are almost the same. This suggests the accurate characterization of groundwater TTD is critical to the accuracy and reliability of simulated MTT, and the uncertainty in soil water TTs is almost irrelevant to the simulated MTT. Unfortunately, the simulated groundwater TTD is inevitably subject to parameter uncertainty because the regional hydraulic parameters are typically inferred through model calibration. Many studies also reveal that a calibrated groundwater model cannot be exempted from parameter uncertainty due to the calibration null-space and the model structural error (Moore and Doherty, 2006; Zink et al., 2017; Jing et al., 2019). MTT seems to be an incomplete description of such power-law type TTDs due to the fact that a marginal error in groundwater characterization will dramatically bias the value of MTT. Similarly, the SD of TT is also sensitive to the long tail of TTD. Some recent studies also show that MTT inferred from tracer data may significantly bias from the true MTT due to the nonlinear mixing of tracers with different ages (Kirchner, 2016; Stewart et al., 2017). Our study extends this conclusion from tracer interpretation to explicit numerical modeling.

Although MTT is the most commonly used summary statistics to represent catchment transport processes, we advocate for using multiple summary statistics including the mean, the standard deviation, the median, the interquartile range, and the young water fraction (Kirchner, 2016) to describe catchment TTD. The median and interquartile range of travel times are relatively less error prone to the tailing behavior of catchment TTD, which are more representative of power-law type TTDs than the mean and standard deviation. The young water fraction (i.e., the fraction of runoff younger than a certain threshold – say 2-3 months) is immune to the aggregation error (Kirchner, 2016; Stewart et al., 2017). Although not used in this study, young water fraction proves to be effective in reducing the uncertainty in tracer-based TTD predictions (Stewart et al., 2017; Lutz et al., 2018).

4.5. Advantages and limitations of current modeling framework

The proposed modeling framework allows for different spatial discretizations of the domain and temporal resolutions in soil zone and groundwater aquifer. For example, it allows daily simulation of soil-zone dynamics and monthly simulation of saturated groundwater flow, as well as the coarse spatial resolution of climate forcing and fine spatial resolution of terrain. In contrast, fully physically-based models (e.g., HydroGeoSphere, ParFlow, and CATHY) explicitly solve partial differential equations of surface flow and unsaturated-saturated groundwater flow, therefore require continuous discretization of mesh, meaning that the size of the grid can essentially vary in several magnitudes in the same mesh due to the fine-scale features in the soil zone and the coarse-scale aquifer properties. This may cause huge numerical expense and potential numerical oscillation when dealing with complex large-scale real-world catchments (Paniconi and Putti, 2015). Our method allows different grid sizes in soil zone and groundwater aquifer because these two compartments are simulated in two models and dynamically linked through model interfaces. Therefore, the proposed mHM-OGS model provides better numerical stability than those of Richard's equation-based models.

Notwithstanding the aforementioned advantages, the proposed modeling framework also has certain limitations. First, the current framework relies on the hydrologic partition function that partitions the subsurface into functional zones. This approach has been extensively used to investigate the transport of environmental tracers and to derive catchment TTDs (Benettin et al., 2015; Birkel et al., 2015). The accurate estimation of internal fluxes (e.g., groundwater recharge) is critical to the simulated TTDs in this approach (Jing et al., 2019). This partitioning is straightforward and flexible, therefore it enables the coupling of flux tracking approach and particle tracking approach and the integrated modeling of catchment TTD. However, it is a conceptual assumption and suffers from a lack of physical interpretation. While a fully physically-based modeling approach to catchment flow and transport processes is more sound in this respect (Kaandorp et al., 2018; Yang et al., 2018), it does suffer from the high computational and data demand, and uncertain parameterizations and numerical instabilities for their application in a real-world mesoscale catchment. Conversely, the approach proposed in this study is computationally efficient, parsimonious, and numerically robust.

The second limitation of this study lies in the exclusive use of hydrometric data for the model evaluation (McDonnell and Beven, 2014). Isotope or conservative tracer concentrations prove to be beneficial in testing and validating the flux-tracking and particle-tracking models (Eberts et al., 2012; Davies et al., 2013; Remondi et al., 2018; Lutz et al., 2018). However, it is difficult to integrate tracer datasets into the numerical setup in the study area because long-term high-frequency measurements of tracer concentrations for groundwater and streams are required, which are unfortunately not available yet. Even if available, a reasonable reconstruction of distributed inputs might be problematic for a catchment of this size. The absence of the tracer datasets implies that the simulated TTDs and the summary statistics are subject to a certain degree of uncertainty. Other avenues to test these integrated modeling approach lie in utilizing model to capture observed dynamics of non-conservative solutes like NO_3-N nitrate. However such efforts require integration and tracking of both hydrologic and biogeochemical processes. There has been some recent efforts utilizing the valuable flux-tracking TTDs approach within the mHM modeling framework for the solute transport modeling (Kumar et al., 2020; Nguyen et al., 2020).

This study by considering spatially explicit TTDs has important implications for the assessment of nonpoint-source contamination. It provides additional information on the spatial pattern in grid-scale water TTDs, which can not be revealed by a lumped, catchment-scale tracer experiment. The particle tracking model can be used to interpret the tracer data with better accuracy compared to the lumped parameter model (Leray et al., 2016;

Danesh-Yazdi et al., 2018). Therefore, the joint investigation by integrating the tracer experiment and numerical modeling is strongly recommended for future studies.

5. Conclusions

This study proposes a novel modeling framework to estimate the water TTDs based on flux tracking in a near-surface, soil-water compartment, and particle tracking in the deeper groundwater compartment. We use the proposed approach to investigate the TTDs in Nägelstedt catchment in central Germany. Based on the hydrologic partition function, the TTDs in soil zone and groundwater aquifer have been studied separately using two different approaches. The TTDs for different hydrologic compartments are integrated as TTDs for the whole subsurface system. This framework facilitates the explicit representation of the groundwater transport process, meanwhile, it is also flexible and computationally robust.

The simulation results reveal strong spatial variability in both shapes and scales of grid-scale groundwater TTDs in the study area. Specifically, grid-scale groundwater TTDs in different grid cells vary significantly in both shape and scale, which is attributed to the stratigraphy and the heterogeneity in the topographic properties and the spatially variable organizations of groundwater flow pathways. Simulated grid-scale water TTDs have great implications in assessing the nonpoint-source contamination in central Germany.

This study also reveals the contrasting temporal variability in TTs in different hydrological components. We observe a seasonal behavior in soil-water TTs and a relatively stable groundwater TTs, indicating the contrasting sensitivities of soil-water and groundwater transport processes to climate forcings. The temporal variability decreases with the time in the Nägelstedt catchment, indicating the highly variable distributions of soil-water TTs and the almost constant distribution of groundwater TTs.

Simulation results suggest a power-law type and fractal behavior of catchment TTD. It further shows that the predictive uncertainty in catchment MTT is dominated by the contribution from groundwater uncertainty and almost immune to the uncertainty in the soil zone. The power-law shape catchment TTD makes the MTT extremely vulnerable to biased groundwater characterization. A joint description of catchment TTD using multiple summary statistics is strongly recommended to characterize catchment transport processes.

Acknowledgements

We thank the Editor Paolo D'Odorico and two reviewers (Simone Fatichi and an anonymous reviewer) for their constructive feedback. For this study, Miao Jing, received financial support from the Deutsche Forschungsgemeinschaft via Sonderforschungsbereich CRC 1076 AquaDiva, and Falk Heße from the Deutsche Forschungsgemeinschaft via Grant Number: HE-7028-1/2. The authors acknowledge Sabine Sattler for providing the geological data, as well various other data providers including DWD, TLUG, JRC, GRDC, and BGR.

Data availability statement

The coupled mHM-OGS model can be freely downloaded and distributed through the following online repository: `https://doi.org/10.5281/zenodo.1248005`.

Appendix A. Evaluation of mHM-OGS model using long-term observations of distributed groundwater levels

To evaluate the performance of the mHM-OGS model in simulating groundwater head dynamics, we compare the simulated groundwater heads to the long-term records in many spatially distributed monitoring wells. For the sake of simplicity, we display the results of simulated and observed groundwater levels in four monitoring wells (Figure A.13). The spatial locations of these monitoring wells and more details of the model evaluation can be found in Jing et al. (2018).

Appendix B. Parameter uncertainty in hydraulic conductivity of groundwater aquifer

To assess the influence of parameter uncertainty in hydraulic conductivity on the simulated groundwater travel times, we generate an ensemble of hydraulic conductivity fields using the null-space Monte Carlo (NSMC) method. Employing this method, we generate 400 hydraulic conductivity fields that are all compatible with the observed discharge and groundwater levels (Figure B.14). Figure B.14 shows the range of hydraulic conductivity for 8 main geological units in the groundwater aquifer. The hydraulic conductivities in the less permeable Muschelkalk formations (mo2, mm2, and mu2) are tied with the corresponding more-permeable formations (mo1, mm1, and mu1)

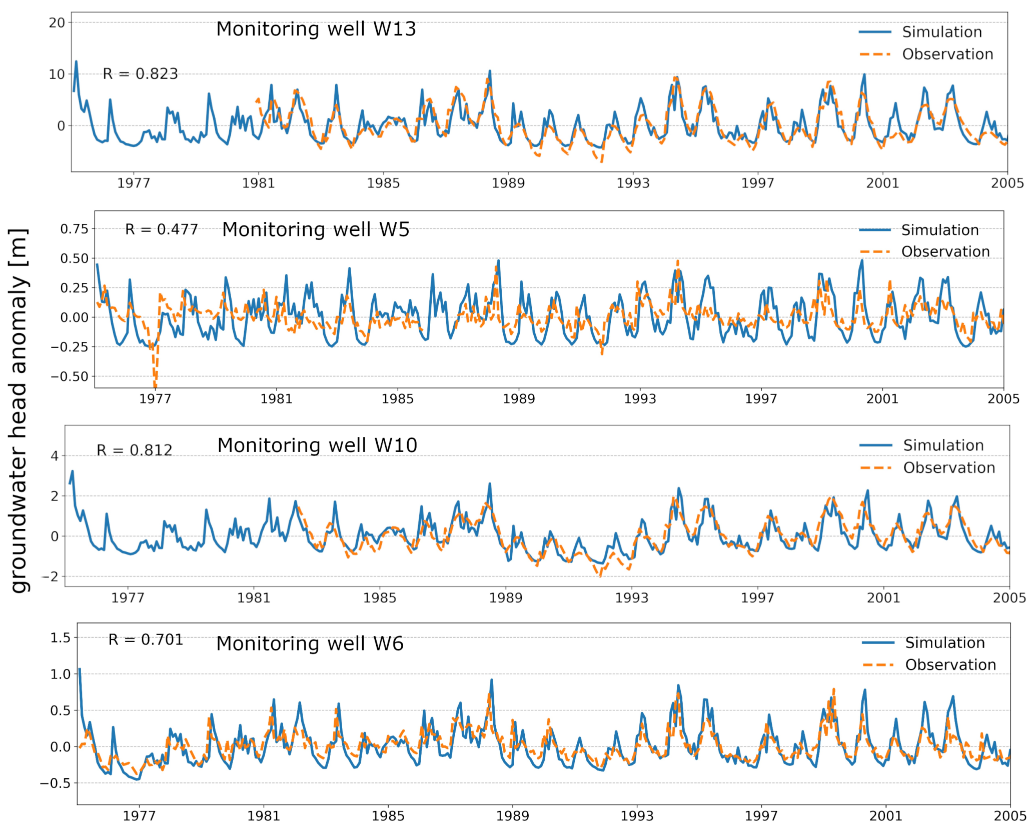

Figure A.13: Model evaluation: simulated and observed groundwater levels at distributed groundwater monitoring wells (Jing et al., 2018). A higher Pearson correlation coefficient (R) indicates a better capture of fluctuations in groundwater levels.

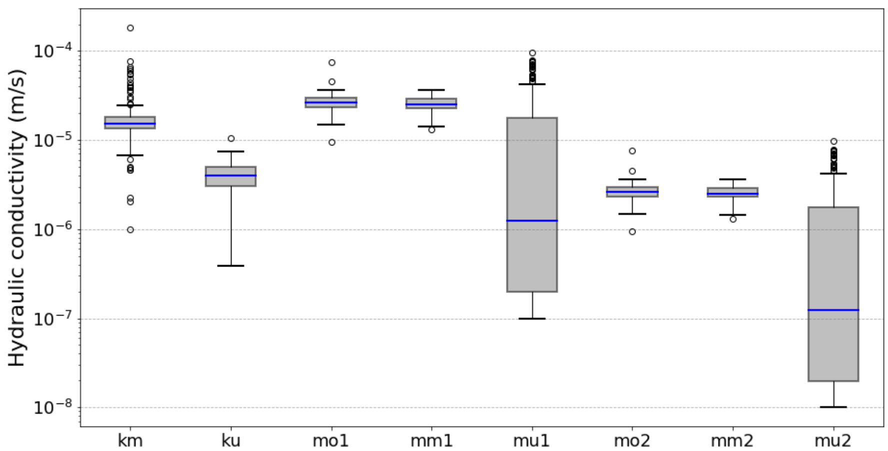

Figure B.14: Boxplot of 400 hydraulic conductivity fields that are all compatible with the observed discharge and groundwater levels.

with a factor of 0.1. This figure indicates that the deepest Lower Muschelkalk formation (mu) has the largest uncertainty. This indicates a low sensitivity of the hydraulic conductivity in this unit to groundwater level observations.

References

Abrams, D., Haitjema, H., 2018. How Aquifer Characteristics of a Watershed Affect Transit Time Distributions of Groundwater. Groundwater 56, 517–520. doi:10.1111/gwat.12788.

Ameli, A.A., Amvrosiadi, N., Grabs, T., Laudon, H., Creed, I.F., McDonnell, J.J., Bishop, K., 2016. Hillslope permeability architecture controls on subsurface transit time distribution and flow paths. Journal of Hydrology 543, 17–30. URL: http://dx.doi.org/10.1016/j.jhydrol.2016.04.071, doi:10.1016/j.jhydrol.2016.04.071.

Benettin, P., Kirchner, J.W., Rinaldo, A., Botter, G., 2015. Modeling chloride transport using travel time distributions at Plynlimon, Wales. Water Resources Research , 3259–3276doi:10.1002/2014WR016600, arXiv:2014WR016600.

Benettin, P., Queloz, P., Bensimon, M., McDonnell, J.J., Rinaldo, A., 2019. Velocities, residence times, tracer breakthroughs in a vegetated lysimeter: A multitracer experiment. Water Resources Research 55, 21–33. URL: https://agupubs.onlinelibrary.wiley.com/doi/abs/10.1029/2018WR023894, doi:10.1029/2018WR023894.

Beven, K., 1989. Interflow. Springer Netherlands, Dordrecht. pp. 191–219. URL: https://doi.org/10.1007/978-94-009-2352-2_7, doi:10.1007/978-94-009-2352-2_7.

Birkel, C., Soulsby, C., Tetzlaff, D., 2011. Modelling catchment-scale water storage dynamics: Reconciling dynamic storage with tracer-inferred passive storage. Hydrological Processes 25, 3924–3936. doi:10.1002/hyp.8201.

Birkel, C., Soulsby, C., Tetzlaff, D., 2015. Conceptual modelling to assess how the interplay of hydrological connectivity, catchment storage and tracer dynamics controls nonstationary water age estimates. Hydrological Processes 29, 2956–2969. URL: https://onlinelibrary.wiley.com/doi/abs/10.1002/hyp.10414, doi:10.1002/hyp.10414, arXiv:https://onlinelibrary.wiley.com/doi/pdf/10.1002/hyp.10414.

Böhlke, J.K., Denver, J.M., 1995. Combined use of groundwater dating, chemical, and isotopic analyses to resolve the history and fate of nitrate contamination in two agricultural watersheds, atlantic coastal plain, maryland. Water Resources Research 31, 2319–2339. URL: https://agupubs.onlinelibrary.wiley.com/doi/abs/10.1029/95WR01584, doi:10.1029/95WR01584.

Botter, G., Bertuzzo, E., Rinaldo, A., 2010. Transport in the hydrologic response: Travel time distributions, soil moisture dynamics, and the old water paradox. Water Resources Research 46, 1–18. doi:10.1029/2009WR008371.

Botter, G., Bertuzzo, E., Rinaldo, A., 2011. Catchment residence and travel time distributions: The master equation. Geophysical Research Letters 38, 1–6. doi:10.1029/2011GL047666.

Cardenas, M.B., 2007. Potential contribution of topography-driven regional groundwater flow to fractal stream chemistry: Residence time distribution analysis of Tóth flow. Geophysical Research Letters 34, 1–5. doi:10.1029/2006GL029126.

Cartwright, I., Cendón, D., Currell, M., Meredith, K., 2017. A review of radioactive isotopes and other residence time tracers in understanding groundwater recharge: Possibilities, challenges, and limitations. Journal of Hydrology 555, 797–811. URL: http://linkinghub.elsevier.com/retrieve/pii/S0022169417307291, doi:10.1016/j.jhydrol.2017.10.053.

Cartwright, I., Morgenstern, U., 2015. Transit times from rainfall to baseflow in headwater catchments estimated using tritium: The Ovens River, Australia. Hydrology and Earth System Sciences 12, 5427–5463. doi:10.5194/hessd-12-5427-2015.

Cornaton, F.J., 2012. Transient water age distributions in environmental flow systems: The time-marching Laplace transform solution technique. Water Resources Research 48, 1–17. doi:10.1029/2011WR010606, arXiv:1109.3133.

Danesh-Yazdi, M., Klaus, J., Condon, L.E., Maxwell, R.M., 2018. Bridging the gap between numerical solutions of travel time distributions and analytical storage selection functions. Hydrological Processes 32, 1063–1076. URL: http://doi.wiley.com/10.1002/hyp.11481, doi:10.1002/hyp.11481.

Davies, J., Beven, K., 2012. Comparison of a multiple interacting pathways model with a classical kinematic wave subsurface flow solution. Hydrological Sciences Journal 57, 203–216. doi:10.1080/02626667.2011.645476.

Davies, J., Beven, K., Rodhe, A., Nyberg, L., Bishop, K., 2013. Integrated modeling of flow and residence times at the catchment scale with multiple interacting pathways. Water Resources Research 49, 4738–4750. doi:10.1002/wrcr.20377.

Eberts, S.M., Böhlke, J.K., Kauffman, L.J., Jurgens, B.C., 2012. Comparison of particle-tracking and lumped-parameter age-distribution models for evaluating vulnerability of production wells to contamination. Hydrogeology Journal 20, 263–282. doi:10.1007/s10040-011-0810-6.

Engdahl, N.B., 2017. Transient effects on confined groundwater age distributions: Considering the necessity of time-dependent simulations. Water Resources Research 53, 7332–7348. doi:10.1002/2016WR019916, arXiv:2014WR016527.

Engdahl, N.B., Maxwell, R.M., 2015. Quantifying changes in age distributions and the hydrologic balance of a high-mountain watershed from climate induced variations in recharge. Journal of Hydrology 522, 152–162. URL: http://dx.doi.org/10.1016/j.jhydrol.2014.12.032, doi:10.1016/j.jhydrol.2014.12.032.

Fenicia, F., Savenije, H.H., Matgen, P., Pfister, L., 2006. Is the groundwater reservoir linear? Learning from data in hydrological modelling. Hydrology and Earth System Sciences 10, 139–150. doi:10.5194/hess-10-139-2006.

Fiori, A., Russo, D., 2008. Travel time distribution in a hillslope: Insight from numerical simulations. Water Resources Research 44, 1–14. doi:10.1029/2008WR007135.

Fischer, T., Naumov, D., Sattler, S., Kolditz, O., Walther, M., 2015. GO2OGS 1.0: A versatile workflow to integrate complex geological information with fault data into numerical simulation models. Geoscientific Model Development 8, 3681–3694. doi:10.5194/gmd-8-3681-2015.

Gleeson, T., Befus, K.M., Jasechko, S., Luijendijk, E., Cardenas, M.B., 2016. The global volume and distribution of modern groundwater. Nature Geoscience 9, 161–164. doi:10.1038/ngeo2590.

Harman, C.J., 2015. Time-variable transit time distributions and transport: Theory and application to storage-dependent transport of chloride in a watershed. Water Resources Research 51, 1–30. doi:10.1002/2014WR015707, arXiv:2014WR016527.

Heße, F., Zink, M., Kumar, R., Samaniego, L., Attinger, S., 2017. Spatially distributed characterization of soil-moisture dynamics using travel-time distributions. Hydrology and Earth System Sciences 21, 549–570. URL: http://www.hydrol-earth-syst-sci.net/21/549/2017/, doi:10.5194/hess-21-549-2017.

Hrachowitz, M., Savenije, H., Bogaard, T.A., Tetzlaff, D., Soulsby, C., 2013. What can flux tracking teach us about water age distribution patterns and their temporal dynamics? Hydrology and Earth System Sciences 17, 533–564. doi:10.5194/hess-17-533-2013.

Hrachowitz, M., Soulsby, C., Tetzlaff, D., Malcolm, I.A., Schoups, G., 2010. Gamma distribution models for transit time estimation in catchments: Physical interpretation of parameters and implications for time-variant transit time assessment. Water Resources Research 46. doi:10.1029/2010WR009148.

Jing, M., Heße, F., Kumar, R., Kolditz, O., Kalbacher, T., Attinger, S., 2019. Influence of input and parameter uncertainty on the prediction of catchment-scale groundwater travel time distributions. Hydrology and Earth System Sciences 23, 171–190. URL: https://www.hydrol-earth-syst-sci.net/23/171/2019/, doi:10.5194/hess-23-171-2019.

Jing, M., Heße, F., Kumar, R., Wang, W., Fischer, T., Walther, M., Zink, M., Zech, A., Samaniego, L., Kolditz, O., Attinger, S., 2018. Improved regional-scale groundwater representation by the coupling of the mesoscale Hydrologic Model (mHM v5.7) to the groundwater model OpenGeoSys (OGS). Geoscientific Model Development 11, 1989–2007. URL: https://www.geosci-model-dev.net/11/1989/2018/, doi:10.5194/gmd-11-1989-2018.

Kaandorp, V.P., de Louw, P.G.B., van der Velde, Y., Broers, H.P., 2018. Transient Groundwater Travel Time Distributions and Age-Ranked Storage-Discharge Relationships of Three Lowland Catchments. Water Resources Research , 1–18URL: http://doi.wiley.com/10.1029/2017WR022461, doi:10.1029/2017WR022461.

Kalbacher, T., Delfs, J.O., Shao, H., Wang, W., Walther, M., Samaniego, L., Schneider, C., Kumar, R., Musolff, A., Centler, F., Sun, F., Hildebrandt, A., Liedl, R., Borchardt, D., Krebs, P., Kolditz, O., 2012. The IWAS-ToolBox: Software coupling for an integrated water resources management. Environmental Earth Sciences 65, 1367–1380. doi:10.1007/s12665-011-1270-y.

Kirchner, J.W., 2016. Aggregation in environmental systems-Part 1: Seasonal tracer cycles quantify young water fractions, but not mean transit times, in spatially heterogeneous catchments. Hydrology and Earth System Sciences 20, 279–297. doi:10.5194/hess-20-279-2016.

Kirchner, J.W., Feng, X., Neal, C., 2000. Fractal stream chemistry and its implications for contaminant transport in catchments. Nature 403, 524. URL: https://doi.org/10.1038/35000537, doi:10.1038/35000537.

Koh, E.H., Lee, E., Kaown, D., Green, C.T., Koh, D.C., Lee, K.K., Lee, S.H., 2018. Comparison of groundwater age models for assessing nitrate loading, transport pathways, and management options in a complex aquifer system. Hydrological Processes 32, 923–938. doi:10.1002/hyp.11465.

Kohlhepp, B., Lehmann, R., Seeber, P., Küsel, K., Trumbore, S.E., Totsche, K.U., 2017. Aquifer configuration and geostructural links control the groundwater quality in thin-bedded carbonate-siliciclastic alternations of the Hainich CZE, central Germany. Hydrology and Earth System Sciences 21, 6091–6116. doi:10.5194/hess-21-6091-2017.

Kolditz, O., Bauer, S., Bilke, L., Böttcher, N., Delfs, J.O., Fischer, T., Görke, U.J., Kalbacher, T., Kosakowski, G., McDermott, C.I., Park, C.H., Radu, F., Rink, K., Shao, H., Shao, H.B., Sun, F., Sun, Y.Y., Singh, A.K., Taron, J., Walther, M., Wang, W., Watanabe, N., Wu, Y., Xie, M., Xu, W., Zehner, B., 2012. OpenGeoSys: an open-source initiative for numerical simulation of thermo-hydro-mechanical/chemical (THM/C) processes in porous media. Environmental Earth Sciences 67, 589–599. URL: http://link.springer.com/10.1007/s12665-012-1546-x, doi:10.1007/s12665-012-1546-x.

Kottek, M., Grieser, J., Beck, C., Rudolf, B., Rubel, F., 2006. World map of the Köppen-Geiger climate classification updated. Meteorologische Zeitschrift 15, 259–263. doi:10.1127/0941-2948/2006/0130.

Kumar, R., Heße, F., Rao, P.S.C., Musolff, A., Jawitz, J.W., Fleckenstein, J.H., Rakovec, O., Thober, S., Attinger, S., 2020. Strong hydroclimatic controls on vulnerability to subsurface nitrate contamination across Europe. Nature Communications , 1–10URL: http://dx.doi.org/10.1038/s41467-020-19955-8, doi:10.1038/s41467-020-19955-8.

Kumar, R., Samaniego, L., Attinger, S., 2013. Implications of distributed hydrologic model parameterization on water fluxes at multiple scales and locations. Water Resour. Res. 49, 360–379. doi:10.1029/2012WR012195.

Küsel, K., Totsche, K.U., Trumbore, S.E., Lehmann, R., Steinhäuser, C., Herrmann, M., 2016. How Deep Can Surface Signals Be Traced in the Critical Zone? Merging Biodiversity with Biogeochemistry Research in a Central German Muschelkalk Landscape. Frontiers in Earth Science 4, 1–18. URL: http://journal.frontiersin.org/Article/10.3389/feart.2016.00032/abstract, doi:10.3389/feart.2016.00032.

Leray, S., Engdahl, N.B., Massoudieh, A., Bresciani, E., McCallum, J., 2016. Residence time distributions for hydrologic systems: Mechanistic foundations and steady-state analytical solutions. Journal of Hydrology 543, 67–87. URL: http://dx.doi.org/10.1016/j.jhydrol.2016.01.068, doi:10.1016/j.jhydrol.2016.01.068.

Livneh, B., Kumar, R., Samaniego, L., 2015. Influence of soil textural properties on hydrologic fluxes in the mississippi river basin. Hydrological Processes 29, 4638–4655. URL: https://onlinelibrary.wiley.com/doi/abs/10.1002/hyp.10601, doi:https://doi.org/10.1002/hyp.10601, arXiv:https://onlinelibrary.wiley.com/doi/pdf/10.1002/hyp.10601.

Lutz, S.R., Krieg, R., Müller, C., Zink, M., Knöller, K., Samaniego, L., Merz, R., 2018. Spatial Patterns of Water Age: Using Young Water Fractions to Improve the Characterization of Transit Times in Contrasting Catchments. Water Resources Research 54, 4767–4784. doi:10.1029/2017WR022216.

Maxwell, R.M., Condon, L.E., Danesh-Yazdi, M., Bearup, L.A., 2019. Exploring source water mixing and transient residence time distributions of outflow and evapotranspiration with an integrated hydrologic model and lagrangian particle tracking approach. Ecohydrology 12, e2042. URL: https://onlinelibrary.wiley.com/doi/abs/10.1002/eco.2042, doi:https://doi.org/10.1002/eco.2042, arXiv:https://onlinelibrary.wiley.com/doi/pdf/10.1002/eco.2042. e2042 ECO-18-0093.R1.

McCallum, J.L., Cook, P.G., Dogramaci, S., Purtschert, R., Simmons, C.T., Burk, L., 2017. Identifying modern and historic recharge events from tracer-derived groundwater age distributions. Water Resources Research 53, 1039–1056. doi:10.1002/2016WR019839, arXiv:2014WR016527.

McCallum, J.L., Engdahl, N.B., Ginn, T.R., Cook, P.G., 2014. Nonparametric estimation of groundwater residence time distributions: What can environmental tracer data tell us about groundwater residence time? Water Resources Research 50, 2022–2038. doi:10.1002/2013WR014974, arXiv:2014WR016527.

McDonnell, J.J., Beven, K., 2014. Debates—the future of hydrological sciences: A (common) path forward? a call to action aimed at understanding velocities, celerities and residence time distributions of the headwater hydrograph. Water Resources Research 50, 5342–5350. URL: https://agupubs.onlinelibrary.wiley.com/doi/abs/10.1002/2013WR015141, doi:https://doi.org/10.1002/2013WR015141, arXiv:https://agupubs.onlinelibrary.wiley.com/doi/pdf/10.1002/2013WR015141.

McDonnell, J.J., McGuire, K., Aggarwal, P., Beven, K.J., Biondi, D., Destouni, G., Dunn, S., James, A., Kirchner, J., Kraft, P., Lyon, S., Maloszewski, P., Newman, B., Pfister, L., Rinaldo, A., Rodhe, A., Sayama, T., Seibert, J., Solomon, K., Soulsby, C., Stewart, M., Tetzlaff, D., Tobin, C., Troch, P., Weiler, M., Western, A., Wörman, A., Wrede, S., 2010. How old is streamwater? Open questions in catchment transit time conceptualization, modelling and analysis. Hydrological Processes 24, 1745–1754. doi:10.1002/hyp.7796.

McGuire, K.J., McDonnell, J.J., 2006. A review and evaluation of catchment transit time modeling. Journal of Hydrology 330, 543–563. doi:10.1016/j.jhydrol.2006.04.020.

McGuire, K.J., Weiler, M., McDonnell, J.J., 2007. Integrating tracer experiments with modeling to assess runoff processes and water transit times. Advances in Water Resources 30, 824–837. doi:10.1016/j.advwatres.2006.07.004.

McMillan, H., Tetzlaff, D., Clark, M., Soulsby, C., 2012. Do time-variable tracers aid the evaluation of hydrological model structure? A multimodel approach. Water Resources Research 48. doi:10.1029/2011WR011688.

Molnat, J., Gascuel-Odoux, C., 2002. Modelling flow and nitrate transport in groundwater for the prediction of water travel times and of consequences of land use evolution on water quality. Hydrological Processes 16, 479–492. doi:10.1002/hyp.328.

Moore, C., Doherty, J., 2006. The cost of uniqueness in groundwater model calibration. Advances in Water Resources 29, 605–623. doi:10.1016/j.advwatres.2005.07.003.

Mueller, C., Zink, M., Samaniego, L., Krieg, R., Merz, R., Rode, M., Knöller, K., 2016. Discharge Driven Nitrogen Dynamics in a Mesoscale River Basin As Constrained by Stable Isotope Patterns. Environmental Science & Technology 50, 9187–9196. URL: https://doi.org/10.1021/acs.est.6b01057, doi:10.1021/acs.est.6b01057.

Nguyen, T.V., Kumar, R., Lutz, S.R., Musolff, A., Yang, J., Fleckenstein, J.H., 2020. Modeling nitrate export from a mesoscale catchment using storage selection functions. Water Resources Research n/a, e2020WR028490. URL: https://agupubs.onlinelibrary.wiley.com/doi/abs/10.1029/2020WR028490, doi:https://doi.org/10.1029/2020WR028490, arXiv:https://agupubs.onlinelibrary.wiley.com/doi/pdf/10.1029/2020WR028490.

Niemi, A.J., 1977. Residence time distributions of variable flow processes. The International Journal of Applied Radiation and Isotopes 28, 855–860. URL: http://www.sciencedirect.com/science/article/pii/0020708X77900266.

Paniconi, C., Putti, M., 2015. Physically based modeling in catchment hydrology at 50: Survey and outlook. Water Resources Research 51, 7090–7129. URL: http://dx.doi.org/10.1002/2015WR017780, doi:10.1002/2015WR017780, arXiv:2014WR016527.

Park, C.H., Beyer, C., Bauer, S., Kolditz, O., 2008. Using global node-based velocity in random walk particle tracking in variably saturated porous media: Application to contaminant leaching from road constructions. Environmental Geology 55, 1755–1766. doi:10.1007/s00254-007-1126-7.

Rakovec, O., Kumar, R., Mai, J., Cuntz, M., Thober, S., Zink, M., Attinger, S., Schäfer, D., Schrön, M., Samaniego, L., 2016. Multiscale and multivariate evaluation of water fluxes and states over European river basins. J. Hydrometeorol. 17, 287–307.

Remondi, F., Botter, M., Burlando, P., Fatichi, S., 2019. Variability of transit time distributions with climate and topography: A modelling approach.

Journal of Hydrology 569, 37–50. URL: https://doi.org/10.1016/j.jhydrol.2018.11.011, doi:10.1016/j.jhydrol.2018.11.011.

Remondi, F., Kirchner, J.W., Burlando, P., Fatichi, S., 2018. Water Flux Tracking With a Distributed Hydrological Model to Quantify Controls on the Spatiotemporal Variability of Transit Time Distributions. Water Resources Research 54, 3081–3099. doi:10.1002/2017WR021689.

Rinaldo, A., Benettin, P., Harman, C.J., Hrachowitz, M., McGuire, K.J., van der Velde, Y., Bertuzzo, E., Botter, G., 2015. Storage selection functions: A coherent framework for quantifying how catchments store and release water and solutes. Water Resources Research 51, 4840–4847. URL: https://agupubs.onlinelibrary.wiley.com/doi/abs/10.1002/2015WR017273, doi:10.1002/2015WR017273.

Rinaldo, A., Beven, K.J., Bertuzzo, E., Nicotina, L., Davies, J., Fiori, A., Russo, D., Botter, G., 2011. Catchment travel time distributions and water flow in soils. Water Resources Research 47, 1–13. doi:10.1029/2011WR010478.

de Rooij, R., Graham, W., Maxwell, R.M., 2013. A particle-tracking scheme for simulating pathlines in coupled surface-subsurface flows. Advances in Water Resources 52, 7–18. URL: http://dx.doi.org/10.1016/j.advwatres.2012.07.022, doi:10.1016/j.advwatres.2012.07.022.

Samaniego, L., Kumar, R., Attinger, S., 2010. Multiscale parameter regionalization of a grid-based hydrologic model at the mesoscale. Water Resources Research 46, n/a–n/a. URL: http://doi.wiley.com/10.1029/2008WR007327, doi:10.1029/2008WR007327.

Samaniego, L., Thober, S., Kumar, R., Wanders, N., Rakovec, O., Pan, M., Zink, M., Sheffield, J., Wood, E.F., Marx, A., 2018. Anthropogenic warming exacerbates European soil moisture droughts. Nature Climate Change 8, 421–426. URL: http://dx.doi.org/10.1038/s41558-018-0138-5, doi:10.1038/s41558-018-0138-5.

Sprenger, M., Stumpp, C., Weiler, M., Aeschbach, W., Allen, S.T., Benettin, P., Dubbert, M., Hartmann, A., Hrachowitz, M., Kirchner, J.W., McDonnell, J.J., Orlowski, N., Penna, D., Pfahl, S., Rinderer, M., Rodriguez, N., Schmidt, M., Werner, C., 2019. The demographics of water: A review of water ages in the critical zone. Reviews of Geophysics URL: https://onlinelibrary.wiley.com/doi/abs/10.1029/2018RG000633, doi:10.1029/2018RG000633.

Stewart, M.K., Morgenstern, U., Gusyev, M.A., Maloszewski, P., 2017. Aggregation effects on tritium-based mean transit times and young water fractions in spatially heterogeneous catchments and groundwater systems. HYDROLOGY AND EARTH SYSTEM SCIENCES 21, 4615–4627. doi:{10.5194/hess-21-4615-2017}.

Stewart, M.K., Morgenstern, U., Mcdonnell, J.J., Pfister, L., 2012. The 'hidden streamflow' challenge in catchment hydrology: A call to action for stream water transit time analysis. Hydrological Processes 26, 2061–2066. doi:10.1002/hyp.9262.

Sun, F., Shao, H., Kalbacher, T., Wang, W., Yang, Z., Huang, Z., Kolditz, O., 2011. Groundwater drawdown at Nankou site of Beijing Plain: model development and calibration. Environmental Earth Sciences 64, 1323–1333. URL: http://link.springer.com/10.1007/s12665-011-0957-4, doi:10.1007/s12665-011-0957-4.

Thober, S., Kumar, R., Wanders, N., Marx, A., Pan, M., Rakovec, O., Samaniego, L., Sheffield, J., Wood, E.F., Zink, M., 2018. Multi-model ensemble projections of european river floods and high flows at 1.5, 2, and 3 degrees global warming. Environmental Research Letters 13, 014003. URL: https://doi.org/10.1088\%2F1748-9326\%2Faa9e35, doi:10.1088/1748-9326/aa9e35.

Tonkin, M., Doherty, J., 2009. Calibration-constrained Monte Carlo analysis of highly parameterized models using subspace techniques. Water Resources Research 45, 1–17. doi:10.1029/2007WR006678.

Van Meter, K.J., Basu, N.B., Van Cappellen, P., 2017. Two centuries of nitrogen dynamics: Legacy sources and sinks in the Mississippi and Susquehanna River Basins. Global Biogeochemical Cycles 31, 2–23. doi:10.1002/2016GB005498.

Van Meter, K.J., Van Cappellen, P., Basu, N.B., 2018. Legacy nitrogen may prevent achievement of water quality goals in the Gulf of Mexico. Science 360, 427–430.

Wechsung, F., Kaden, S., Behrendt, H., Klöcking, B. (Eds.), 2008. Integrated Analysis of the Impacts of Global Change on Environment and Society in the Elbe Basin. Schweizerbart Science Publishers, Stuttgart, Germany. URL: http://www.schweizerbart.de/publications/detail/isbn/9783510653041/Wechsung_Integrated_Analysis_of_the_Imp.

Weissmann, G.S., Zhang, Y., LaBolle, E.M., Fogg, G.E., 2002. Dispersion of groundwater age in an alluvial aquifer system. Water Resources Research 38, 16–1–16–13. URL: http://doi.wiley.com/10.1029/2001WR000907, doi:10.1029/2001WR000907.

Yang, J., Heidbüchel, I., Musolff, A., Reinstorf, F., Fleckenstein, J.H., 2018. Exploring the Dynamics of Transit Times and Subsurface Mixing in a Small Agricultural Catchment. Water Resources Research , 2317–2335URL: http://doi.wiley.com/10.1002/2017WR021896, doi:10.1002/2017WR021896.

Zink, M., Kumar, R., Cuntz, M., Samaniego, L., 2017. A high-resolution dataset of water fluxes and states for Germany accounting for parametric uncertainty. Hydrology and Earth System Sciences 21, 1769–1790. URL: http://www.hydrol-earth-syst-sci.net/21/1769/2017/, doi:10.5194/hess-21-1769-2017.

Zink, M., Mai, J., Cuntz, M., Samaniego, L., 2018. Conditioning a hydrologic model using patterns of remotely sensed land surface temperature. Water Resources Research 54, 2976–2998. URL: https://agupubs.onlinelibrary.wiley.com/doi/abs/10.1002/2017WR021346, doi:10.1002/2017WR021346.